



MDOT State Study 287—Evaluation of Ground Penetrating Radar as a Tool in Designing Maintenance and Rehabilitation Projects in Mississippi

L. Allen Cooley, Jr., Ph.D.
Robert L. Varner, P.E.
R. C. Ahlrich, Ph.D., P.E.
Scott Bivings
Burns Cooley Dennis, Inc.

Report Date: 12/18/2019

BURNS COOLEY DENNIS, INC.

GEOTECHNICAL AND MATERIALS ENGINEERING CONSULTANTS

FHWA Technical Report Documentation Page

1. Report No. FHWA/MDOT-RD-20-287	2. Government Accession No.	3. Recipient's Catalog No.	
4. Title and Subtitle Evaluation of Ground Penetrating Radar as a Tool in Designing Maintenance and Rehabilitation Projects in Mississippi		5. Report Date December 18, 2019	
		6. Performing Organization Code 170592	
7. Author(s) L. Allen Cooley, Jr., Ph.D. Robert L. Varner, P.E. R. C. Ahlrich, Ph.D., P.E. Scott Bivings		8. Performing Organization Report No.	
9. Performing Organization Name and Address Mississippi Department of Transportation PO Box 1850 Jackson, MS 39215-1850		10. Work Unit No. (TRAIS)	
		11. Contract or Grant No. SPR-2017(029)/107692-101000	
12. Sponsoring Agency Name and Address		13. Type Report and Period Covered 10/03/2017 – 12/31/2019	
		14. Sponsoring Agency Code	
15. Supplementary Notes			
16. Abstract This research project was conducted to evaluate the ground penetrating radar (GPR) for use as a tool to assist an Engineer in designing maintenance and rehabilitation solutions. GPR testing was conducted on 64 different pavement sections located around the state of Mississippi. GPR traces from 16 of these sections were evaluated in order to compare traces to visible and non-visible distresses. Based upon the conduct of the research, it was concluded that the GPR has the potential for identifying distresses within a pavement structure. Based upon the success of this research, it was recommended that an additional study be conducted to evaluate the remaining 48 pavement sections to further refine the benefits of the GPR.			
17. Key Words Pavements, maintenance & rehabilitation, ground penetrating radar, hot mix asphalt, cementitious stabilized materials		18. Distribution Statement Unclassified	
19. Security Classif. (of this report) Unclassified	20. Security Classif. (of this page) Unclassified	21. No. of Pages 76	22. Price

Disclaimer

Burns Cooley Dennis, Inc. and the Mississippi Department of Transportation do not endorse service providers, products, or manufacturers. Trade names or manufacturers' names appear herein solely because they are considered essential to the purpose of this report.

The contents of this report do not necessarily reflect the views and policies of the sponsor agency.

MDOT Statement of Nondiscrimination

The Mississippi Department of Transportation (MDOT) operates its programs and services without regard to race, color, national origin, sex, age, or disability in accordance with Title VI of the Civil Rights Act of 1964, as amended and related statutes and implementing authorities.

Author Acknowledgments

The authors wish to thank Bill Barstis, MDOT Research Division, for his impetus for the research study and his assistance and guidance throughout the study. In addition, Alex Middleton and Alex Collum, MDOT Research Division, were instrumental in assisting prior to and during site visits in which Ground Penetrating Radar testing was conducted. Members of the MDOT District Maintenance Division are greatly appreciated for providing traffic control on all test sections.

Table of Contents

Disclaimer.....	i
MDOT Statement of Nondiscrimination	ii
Author Acknowledgments	iii
Table of Contents.....	iv
List of Figures	v
List of Tables	vii
List of Abbreviations	viii
Executive Summary.....	ix
Introduction/Background	1
Methodology/Research Approach.....	2
Research Findings and Applications.....	6
Experiences with GPR on Site 4669 Near Woodville, MS	7
<i>Summary</i>	17
Subsurface Anomalies within Full 500-ft GPR Trace Evaluations	17
<i>Stripping in HMA</i>	17
<i>Crack at Bottom of HMA Layer</i>	21
<i>Crack Mid-Depth Within HMA Layer</i>	23
<i>Crack Within CSM Layer</i>	25
<i>Fatigue Cracking Within CSM Layer</i>	27
<i>Interesting Observations from Five Full 500-ft Traces</i>	30
<i>Summary</i>	35
GPR Traces of Visible Distresses	36
<i>GPR Traces for Visible Longitudinal Cracks</i>	37
<i>GPR Traces for Visible Transverse Cracks</i>	46
<i>GPR Traces of Visible Fatigue Cracking</i>	55
<i>Summary</i>	61
Conclusions and Recommendations.....	61
Implementation Plan/Recommendations.....	63
References	63

List of Figures

Figure 1: GPR and Cart Utilized for Testing.....	3
Figure 2: Location of Five Longitudinal GPR Traces	4
Figure 3: GPR Anomaly Identified at Station 2+46 - Section 4669	8
Figure 4: Core Cut at Station 2+46 - Section 4669	9
Figure 5: GPR Anomaly Identified at Station 3+81 – Section 4669.....	10
Figure 6: Core Cut at Station 3+81 – Section 4669	11
Figure 7: GPR Anomaly Identified at Station 4+73 – Section 4669.....	12
Figure 8: Core Cut at Station 4+73 – Section 4669	13
Figure 9: GPR Anomaly in the Longitudinal Direction Between Stations 1+68 and 1+78 – Section 4669..	14
Figure 10: GPR Anomaly in the Transverse Direction at Stations 1+65, 1+69, and 1+78 – Section 4669 ..	15
Figure 11: Cores Cut at Stations 1+69 and 1+78 – Section 4669	16
Figure 12: RWP and RPE Traces from Section 3163 near Station 3+16	18
Figure 13: BWP Trace from Section 4834 near Station 0+19.....	18
Figure 14: RWP Trace from Section 4864 near Station 0+45.....	19
Figure 15: LWP Trace from Section 5244 near Station 0+52	19
Figure 16: LPE Trace from Section 5244 near Station 2+24.....	20
Figure 17: BWP Trace from Section 5230 near Station 3+00.....	20
Figure 18: LWP and BWP Traces from Section 5230 near Station 2+54.....	21
Figure 19: BWP Trace from Section 4784 near Station 1+98.....	22
Figure 20: LPE Trace from Section 4834 near Station 1+02.....	22
Figure 21: LPE Trace from Section 5210 near Station 0+34.....	23
Figure 22: RWP Trace from Section 2580 near Station 0+92.....	24
Figure 23: LWP Trace from Section 3163 near Station 0+12	24
Figure 24: LWP Trace from Section 4588 near Station 3+34	25
Figure 25: LWP Trace from Section 3163 near Station 2+16	25
Figure 26: LPE Trace from Section 4782 near Station 2+86.....	26
Figure 27:RPE Trace from Section 4784 near Station 0+50	26
Figure 28: LPE Trace from Section 5210 near Station 0+58.....	27
Figure 29: RWP Trace from Section 2580 near Station 1+34.....	28
Figure 30: RWP Trace from Section 4588 near Station 3+34.....	28
Figure 31: RWP Trace from Section 5244 near Station 1+00.....	29
Figure 32: RWP and RPE Traces from Section 5249 near Station 3+50	29
Figure 33: RWP Trace from Section 4588 near Station 0+56.....	30
Figure 34: Five Traces from Section 4782 near Station 3+30	31
Figure 35: Photos of Pavement Surface and CSM Layer near Station 3+30 in Section 4782	32
Figure 36: BWP Trace from Section 4782 near Station 3+35.....	33
Figure 37: RPE Trace from Section 4834 near Station 0+70	33
Figure 38: LWP Trace from Section 5210 near Station 0+24	34
Figure 39: LPE and LWP Traces from Section 5230 near Station 2+96.....	35
Figure 40: RPE Trace from Section 5249 near Station 1+25	35
Figure 41: GPR Trace for Longitudinal Crack - Section 4588, Station 1+60	38

Figure 42: Pavement Surface and Core for Longitudinal Crack - Section 4588, Station 1+60	39
Figure 43: GPR Trace for Longitudinal Crack - Section 4864, Station 1+00	40
Figure 44: Pavement Surface and Core for Longitudinal Crack - Section 4864, Station 1+00	41
Figure 45: GPR Trace for Longitudinal Crack - Section 4865, Station 0+12	42
Figure 46: Pavement Surface and Core for Longitudinal Crack - Section 4865, Station 0+12	43
Figure 47: GPR Traces for Longitudinal Crack - Section 5627, Station 2+16.....	44
Figure 48: Pavement Surface and Core for Longitudinal Crack - Section 4865, Station 2+16.....	45
Figure 49: GPR Traces for Transverse Crack - Section 3163, Station 3+91	47
Figure 50: Pavement Surface and Core for Transverse Crack - Section 3163, Station 3+91	48
Figure 51: GPR Traces for Transverse Crack - Section 4782, Station 1+63	49
Figure 52: Pavement Surface and Core from Transverse Crack - Section 4782, Station 1+63	50
Figure 53: GPR Traces for Transverse Crack - Section 4784, Station 0+15	51
Figure 54: Pavement Surface and Core from Transverse Crack - Section 4784, Station 0+15	52
Figure 55: GPR Traces for Transverse Crack - Section 5210, Station 3+75	53
Figure 56: Pavement Surface and Core from Transverse Crack - Section 5210, Station 3+75	54
Figure 57: GPR Traces for Fatigue Cracks - Section 4782, Station 4+65	55
Figure 58: Pavement Surface and Core from Fatigue Cracks - Section 4782, Station 4+65	56
Figure 59: GPR Traces for Fatigue Cracks - Section 5230, Station 1+25	57
Figure 60: Pavement Surface and Core from Fatigue Crack - Section 5230, Station 1+25.....	58
Figure 61: GPR Traces for Fatigue Cracks - Section 5249, Station 0+12	59
Figure 62: Pavement Surface and Core from Fatigue Crack - Section 5249, Station 0+12.....	60

List of Tables

Table 1: Test Sections for Evaluation of Subsurface Distresses with GPR	5
---	---

List of Abbreviations

BCD – Burns Cooley Dennis, Inc.

BWP – Between wheel path

CSM – Cementitiously stabilized material

GPR – Ground penetrating radar

HMA – Hot mix asphalt

LPE – Left pavement edge

LWP – Left wheel path

M & R – Maintenance and rehabilitation

MDOT – Mississippi Department of Transportation

RPE – Right pavement edge

RWP – Right wheel path

Executive Summary

Within today's environment, a large portion of Mississippi Department of Transportation's (MDOT's) construction budget is spent on maintenance and rehabilitation (M&R) of existing pavements. Because of its ability to identify discontinuities within the pavement structure, the ground penetrating radar (GPR) has the potential of identifying pavement distresses that are not visible at the pavement surface. These distresses could include, stripping within asphalt, cracks which have not propagated to the pavement surface, cracking within stabilized sublayers, etc. Any and all of these distresses that are not visible at the pavement surface could potentially affect M&R design techniques. Therefore, a study was needed to evaluate whether GPR could be used as a tool to assist an Engineer in designing M&R solutions.

Field work for this project involved GPR testing on each of 64 pavement test sections included within State Study (SS) No. 263, "Data Collection for Local Calibration of the AASHTOWare Pavement ME Design Performance Models for Mississippi." These pavement sections were selected because they provided a range of pavement performance, pavement structures, materials, and traffic volumes. While at each of the 64 pavement test sections, two general types of GPR traces were obtained. First, GPR testing was conducted in five longitudinal lines along the full 500-ft of the test section. These five longitudinal GPR traces were located outside the wheel path next to the shoulder, within the outside wheel path, mid-lane between the wheel paths, within the inside wheel path, and outside the wheel path next to the longitudinal joint. GPR testing was also conducted on various pavement distresses observed at the pavement surface on each of the 64 test sections. In addition, cores were cut at the location of these visible pavement distresses. Generally, between four and ten visible distresses were evaluated using the GPR and coring at each section.

Using the collected data, three different analyses were conducted for 16 of the 64 sections. First, a case study was conducted for Site 4669 near Woodville, MS. The term case study is used because this section afforded the only opportunity for the evaluation of the five full length traces prior to sampling the section. This opportunity arose because of equipment issues. The second analysis technique involved evaluating the five full length traces from each of the 16 sections to identify trace characteristics that may be subsurface distresses or other issues. The final analysis technique was to evaluate the GPR traces of selected visible distresses. Based upon the data collected and analyses conducted, the following conclusions were provided:

- In the one instance in which the traces were evaluated prior to the sampling of the pavement, the GPR successfully identified subsurface distresses. Subsurface distresses successfully identified included both cracking within the HMA and cracking within the cementitiously stabilized material (CSM) layer.

- Subsurface anomalies identified by the GPR were generally parabolas, areas of alternating shades of gray, distinct lines of darker gray colors, and distortions within the interfaces between layers.
- The GPR identified subsurface anomalies that included both stripping and delamination.
- The GPR identified subsurface anomalies that could potentially be stripping.
- Subsurface anomalies were identified based on GPR traces that indicated cracks that were near the bottom of the HMA layer.
- Subsurface anomalies were identified based on GPR traces that indicated cracks that had either: 1) initiated mid-depth within the HMA or 2) had propagated from the bottom of the HMA layer to mid-depth.
- Subsurface anomalies found within the CSM layers suggested cracks within the CSM layers.
- Distortions within interfaces between layers suggested the potential for fatigue within CSM layers.
- The GPR was successful at identifying cracks visible at the pavement surface.
- The five full length traces proved easier to evaluate than the short traces obtained over the visible distresses. Full length traces allowed for the observation of boundaries of distinguishing anomalies within these long traces as opposed to the shorter traces where distinguishing anomalies often fully encompassed the full length of the shorter traces; i.e., no features within the shorter trace could be interpreted as a boundary between a distressed and non-distressed area of the pavement layer.
- The five full length traces proved easier to evaluate than the short traces obtained over the visible distresses because it allowed a better comparison because anomalies were different than the remaining portion of the traces.
- Based upon the previous conclusions, it is concluded that the GPR does have the potential to assist an Engineer design an M&R treatment.

Based upon the conclusions of this study, the following recommendations are provided:

- Within the current study, GPR traces from 16 of the available 64 pavement sections were evaluated. Because of the success of identifying anomalies within the traces, and the success, where available, of correlating GPR traces to actual subsurface distresses, it is recommended to evaluate the GPR traces from the remaining 48 sections. Both full length and individual surface distress traces should be evaluated. Evaluation of the remaining GPR traces from the remaining 48 sections may provide further evidence of the ability of the GPR to assist an Engineer design an M&R treatment.
- After evaluating the remaining 48 sections, a subset of the sections should be selected for further investigation. To date, only a single section afforded the opportunity to evaluate the traces and then sample the pavements to verify that the

subsurface anomalies were in fact distresses. A minimum of five additional sections should be sampled for verification purposes.

Introduction/Background

Within today's environment, a large portion of Mississippi Department of Transportation's (MDOT's) construction budget is spent on maintenance and rehabilitation (M&R) of existing pavements. In order for MDOT to recommend M&R strategies on a project-level basis, a series of evaluations must take place. First, as-builts must be obtained in order to determine the planned pavement structure. Next, cores must be cut from the pavement in order to evaluate the condition of the paving materials within the pavement structure and determine thicknesses of pavement structure layers. In some instances, the falling weight deflectometer (FWD) is also used to evaluate the strength of the pavement. Once the pavement structure and condition is known, the structural capacity of the pavement section is estimated. Along with traffic estimates, the estimated pavement structural capacity is used to design M&R techniques.

One key component of evaluating the structural capacity of an in-service pavement is accurately determining the condition of the pavement. Pavement condition has two components. First, there are distresses that are visible at the pavement surface. These visible pavement distresses can provide an indication of the mechanism causing the distress. Knowing the mechanism provides a M&R designer an idea of how to minimize future distresses in the future through the design process.

A second component that is more difficult to account for during M&R design is distresses that are not visible at the pavement surface. A distress that is typical in MDOT pavements that is not visible at the pavement surface is asphalt stripping. Because stripping is not observed at the pavement surface, a designer will only know that stripping has occurred if the cores cut during the evaluation process are cut within an area that has experienced stripping.

A tool that could assist an Engineer in selecting the best location(s) for cores when designing M&R techniques is a ground penetrating radar (GPR). Uddin (1) provides an excellent general overview of the basic principles of GPR technology. The following is from Uddin's report:

“Ground penetrating radar (GPR) is a nondestructive geophysical technique that uses electromagnetic waves to evaluate subsurface information. A GPR unit emits a short pulse of electromagnetic energy and is able to determine the presence or absence of a target by examining the reflected energy from that pulse. An electromagnetic trigger pulse is generated in the control unit and sent to the antenna. In the antenna, each trigger pulse is transformed into a bipolar pulse which has higher amplitude than the trigger pulse. Then, the transmitted pulse in the antenna is radiated into the subsurface

and reflected at boundaries of materials with different values of the dielectric constant. The reflected portion of the electromagnetic signal travels back to the antenna. The receiver of the antenna detects the returning signal and sends it to the control unit to form a series of pulses, known as waveform. The part of the signal not reflected continues through the medium until a boundary of different dielectric property is encountered, which causes further reflections. The series of waveforms recorded at the control unit produce an image. The time delay and amplitude of the waves in this image are related to the location and properties of the interfaces and buried objects.”

Because of its ability to identify discontinuities within the pavement structure, the GPR has the potential of identifying pavement distresses that are not visible at the pavement surface. These distresses could include, stripping within asphalt, cracks which have not propagated to the pavement surface, cracking within stabilized sublayers, etc. Any and all of these distresses that are not visible at the pavement surface could potentially affect M&R design techniques. Therefore, a study was needed to evaluate whether GPR could be used as a tool to assist an Engineer in designing M&R solutions.

Methodology/Research Approach

Field work involved GPR testing on each of 64 pavement test sections included within State Study (SS) No. 263, “Data Collection for Local Calibration of the AASHTOWare Pavement ME Design Performance Models for Mississippi.” These pavement sections were selected because they provided a range of pavement performance, pavement structures, materials, and traffic volumes.

A high-performance, single channel GPR data acquisition system was used for testing during this study. The ground-coupled system utilized a 1.6 GHz antenna with a depth of penetration of approximately 18 in. A three-wheeled utility cart was used to hold the small, hand-held GPR trace display and to push the GPR system along the pavement surface (Figure 1).



Figure 1: GPR and Cart Utilized for Testing

Ground-coupled GPR antennas are designed to work in close proximity to the scanned surface. In operation, the antenna becomes coupled to the scanned surface. For the GPR system used during this study, the antenna was kept 0.5 in. or less from the pavement surface. The transmitter-receiver (T-R) offset for the system was 2.3 in. This T-R offset was taken into account for depth calculations by the computer processing software paired with the GPR.

While at each of the 64 pavement test sections, two general types of GPR traces were obtained. First, GPR testing was conducted in five longitudinal lines along the full 500-ft of the test section, as shown in Figure 2. These five longitudinal GPR traces were located outside the wheel path next to the shoulder, within the outside wheel path, mid-lane between the wheel paths, within the inside wheel path, and outside the wheel path next to the longitudinal joint.

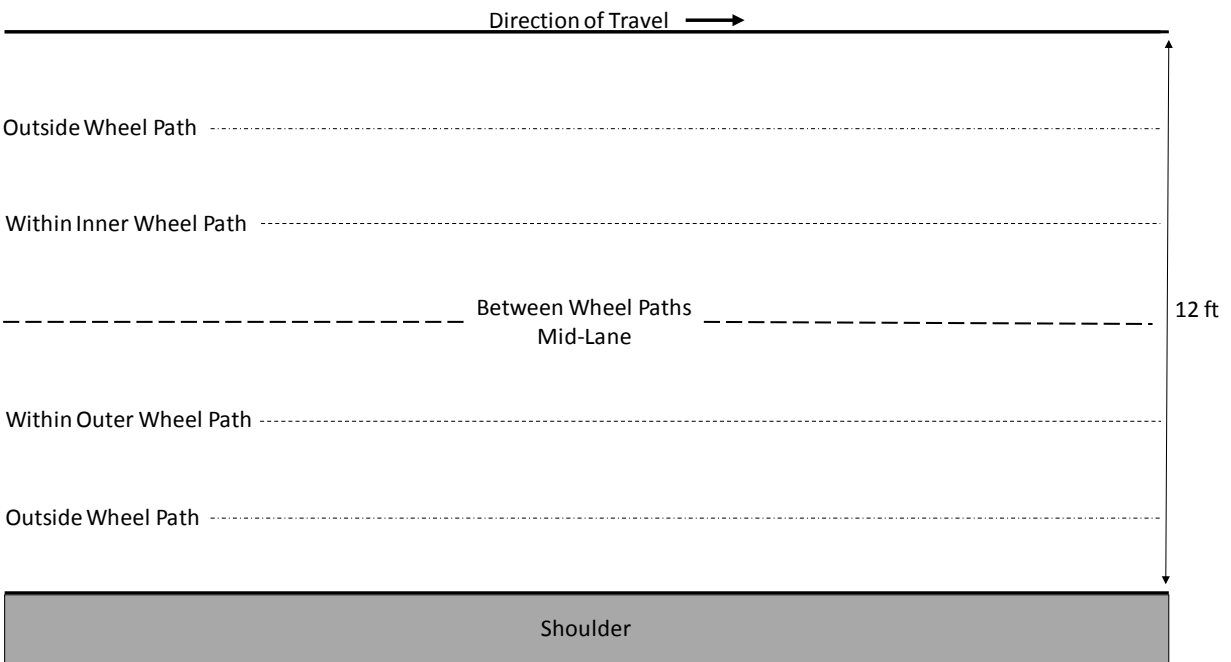


Figure 2: Location of Five Longitudinal GPR Traces

GPR testing was also conducted on various pavement distresses observed at the pavement surface on each of the 64 test sections. In addition, cores were cut at the location of these visible pavement distresses. Generally, between four and ten visible distresses were evaluated using the GPR and coring at each section. The GPR traces were used in an effort to classify given cracks by crack type; i.e.,

- top down fatigue cracks within the hot mix asphalt (HMA) layer,
- bottom up fatigue cracks within the HMA layer,
- shrinkage cracks within an underlying cementitiously stabilized material (CSM) base layer,
- fatigue cracks within an underlying CSM base layer,
- reflection cracks within the HMA layer from the shrinkage and fatigue cracks within the underlying CSM base layer and,
- reflection cracks within an HMA overlay from cracks in underlying original pavement HMA layers.

At the conclusion of the field work, GPR traces were available for 64 500-ft pavement test sections representing the types of typical pavements encountered within Mississippi. In addition, GPR traces were available for visible pavement distresses observed at the pavement surface.

Two primary types of analyses were conducted. These analyses were only conducted on 16 of the 64 pavement test sections. Table 1 presents the 16 pavement test sections in which the analyses were conducted.

Table 1: Test Sections for Evaluation of Subsurface Distresses with GPR

Section	Year Constructed	County	Route
2580	2001	Coahoma	61
3163	2003	Franklin	84
4588	2000	Desoto	302
4669	2001	Wilkinson	61
4782	2001	Clarke	45
4784	1999	Clarke	45
4834	1999	Benton	72
4864	1999	Smith	35
4865	2000	George	63
4902	2000	Attala	43
5210	2002	Winston	19
5230	2002	Winston	15
5244	2003	Franklin	84
5249	2003	Franklin	84
5506	2002	Monroe	45
5627	2002	Desoto	301

The first primary analysis conducted was to identify anomalies within the five full 500-ft traces. Each GPR trace illustrated within Figure 2 were downloaded within its entirety using software provided by the GPR manufacturer. These traces were then exported into CADD. Within CADD, all five traces were placed one on top of each other at equivalent beginning and ends such that the subsurface conditions of the entire pavement width could then be evaluated. A Pavement Engineer with experience interpreting GPR traces then identified discontinuities or anomalies within the GPR traces. Based upon the location and appearance of these anomalies, the probable cause(s) of the anomalies were identified. These anomalies could have been caused by stripping within the hot mix asphalt layer, hot mix asphalt cracking initiating at the bottom of the asphalt layer which has not propagated to the pavement surface, fatigue cracking within stabilized sub-layers, shrinkage cracking within stabilized sub-layers, etc. All of these subsurface distresses could have an impact on the needed M&R of a pavement and, therefore, are important to know when designing M&R strategies. Use of GPR to identify these subsurface distresses would minimize the number of cores required when designing rehabilitation techniques and likely provide more information than just cores and FWD test results.

For the second analysis, GPR traces from the visible pavement distresses were compared to the cores cut from the pavements. The intent of this analysis was to begin correlating GPR traces to typical distresses observed within Mississippi's HMA surfaced pavements.

Research Findings and Applications

The objective of this study was to evaluate the potential use of the GPR device as a tool to assist Engineers in designing M&R treatments. To fully benefit in this purpose, the GPR would need to fulfill two functions. The first function is to provide layer thicknesses for use with FWD analyses. This function has been studied by many researchers and practitioners and has proven successful. The second function would be to identify subsurface pavement areas requiring further evaluation. All roads deteriorate over time. Many of the distresses that develop because of this deterioration are visible at the pavement surface. However, there are also pavement distresses that have not manifested to the pavement surface. If the GPR were successful at identifying these subsurface areas needing further evaluation, it would provide the Engineer beneficial information when designing the M&R treatments. The focus of the analyses conducted within this study is based upon identifying subsurface distresses as well as characterizing GPR traces of visible distresses.

Research findings from this study are divided into three sections. The first section describes a case study in which the five full 500-ft traces were conducted on one of the test sections from SS No. 263. However, before sampling could begin at the test section, a piece of equipment malfunctioned prior to sampling the pavement. Therefore, coring was not conducted on the test section at that time. Once back in the office, the five full 500-ft traces were evaluated in an effort to identify subsurface distresses. Upon returning to the test section, identified potential subsurface distresses were investigated. This first section describes this effort and findings.

The second section of this chapter presents analyses of the full 500-ft section traces in order to identify anomalies that could potentially be subsurface distresses. Observations about the anomalies described within this second section of the chapter are based upon visual inspection of the five full 500-ft traces arranged as shown within Figure 2 (See Figure 34 as an example) for each of the 16 sections shown in Table 1. The five full 500-ft traces have been stored within an FTP site developed for MDOT SS No. 263. Each section evaluated within MDOT SS No. 263 has a distinctive directory within the FTP site. Under the subdirectory entitled “Correlation of GPR to Crack Type or Distress,” the five full 500-ft traces have been stored within a second level subdirectory entitled “MDOT SS No. 287 Full Length Test Section GPR Traces.”

Within the third section, a discussion will be provided that shows the correlations between visible pavement distresses and individual GPR traces. These correlations are based upon the coring of visible distresses from the pavement surface. For each of the visible

distresses cored, GPR traces were taken in a longitudinal and transverse direction prior to coring.

Experiences with GPR on Site 4669 Near Woodville, MS

Burns Cooley Dennis, Inc. (BCD) is currently conducting SS No. 263, Data Collection for Local Calibration of the AASHTOWare Pavement ME Design Performance Models for Mississippi. This is a field and laboratory study designed to document pavement structures in the field and perform laboratory testing to provide data for the calibration of pavement performance models to Mississippi conditions. This study involves sampling 64 pavement sections, each 500 ft in length, from around the state of Mississippi.

Given the amount of time required to perform all activities related to field sampling/testing while at each of the 64 sites, there wasn't time to also thoroughly evaluate the five 500-ft GPR traces collected on the same day the field activities were conducted. However, a single pavement section did allow for the evaluation of GPR traces prior to sampling the pavement and, hence, compare GPR trace anomalies to non-visible distresses/issues within the pavement section. In this case, the five longitudinal GPR traces were obtained at Site 4669 but a piece of equipment malfunctioned resulting in the inability to sample the pavement on the day the traces were obtained. The malfunctioning piece of equipment resulted in discontinuing the sampling for the pavement section.

At the office, the five longitudinal GPR traces from pavement edge to pavement edge were analyzed. This particular pavement section had been rehabilitated with a mill and overlay about a year prior to testing and, therefore, had very few visible distresses at the pavement surface. The combination of GPR traces prior to sampling, evaluation of GPR traces, and finally sampling at a later date provided a unique opportunity to determine the potential cause of some GPR anomalies not visible at the pavement surface.

Analysis of the GPR traces resulted in the identification of numerous anomalies within the pavement section. Due to time constraints during the sampling activities, only a few of these anomalies were further investigated when sampling of the pavement section occurred.

When revisiting the site, measurements were conducted to get close to the anomalies and the GPR was again used to find the specific anomalies. Figure 3 illustrates one of the anomalies that was observed between the wheel paths (BWP) at Station 2+46. As described in Figure 3, the anomaly was a parabola suggesting something occurring in a transverse direction

(longitudinal scan) just below the pavement surface as well as a discontinuity below the hot mix asphalt (HMA) layer. A core was cut at this location which showed an existing crack beginning just below the new HMA pavement surface layer and extending downward (Figure 4). The core cut at this location also revealed a crack within the cementitiously stabilized material (CSM) below the HMA.

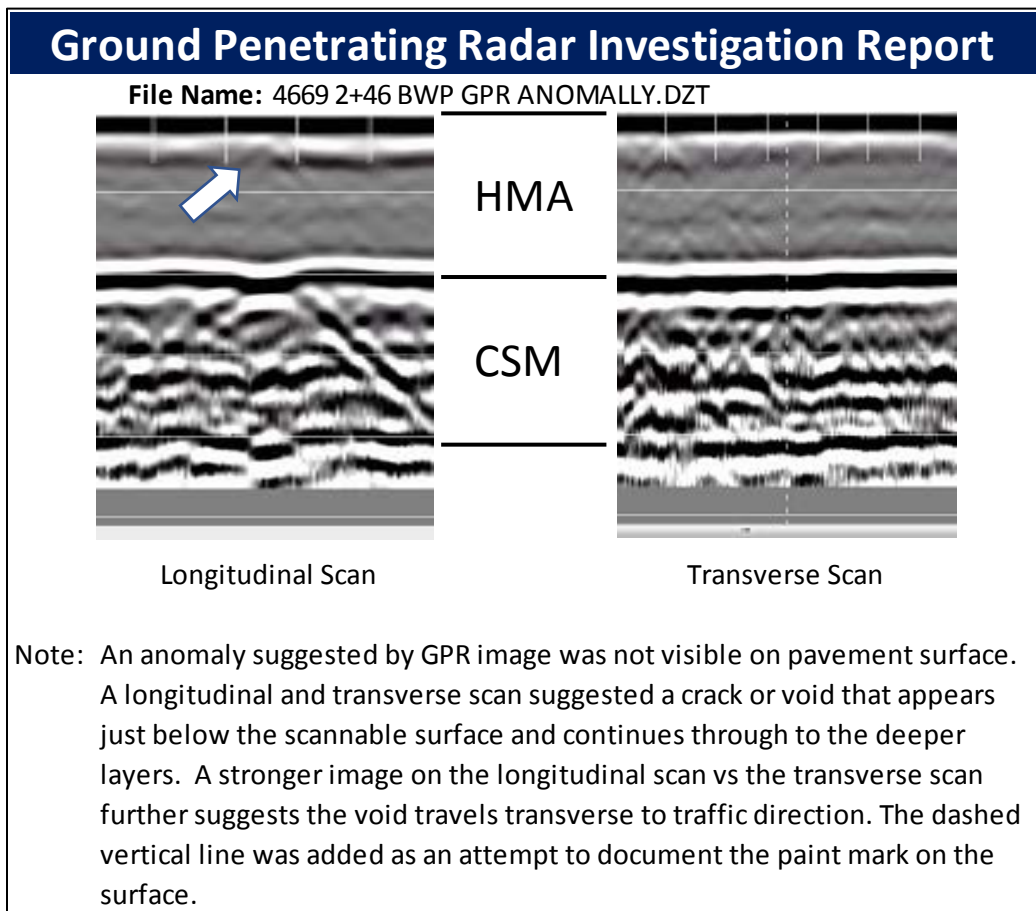
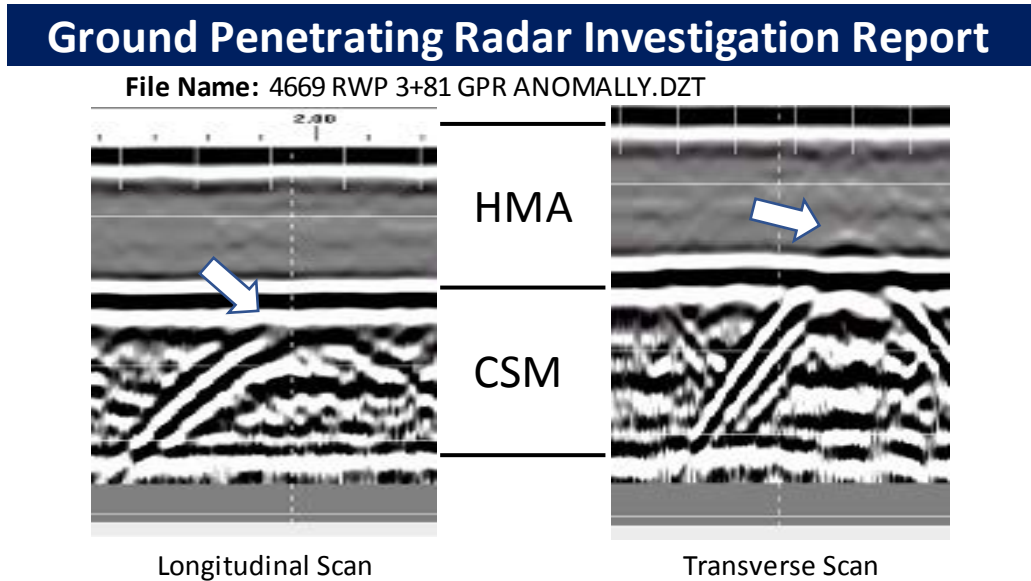


Figure 3: GPR Anomaly Identified at Station 2+46 - Section 4669



Figure 4: Core Cut at Station 2+46 - Section 4669

Figure 5 illustrates the GPR trace for an anomaly located in the right wheel path (RWP) at Station 3+81. As shown in Figure 5, a parabola indicating an anomaly was identified near the bottom of the HMA layer extending downward into the structure. A core was cut at this location (Figure 6). Evaluation of the core did not indicate the cause of the anomaly. A second core was not cut due to time constraints. Whether the anomaly was a false-positive or the core was cut in the wrong location is not known.



Note: GPR suggested an anomaly below the HMA that was not visible at the pavement surface. An exploratory core was made, with no crack found. Closer examination of the scan, (particularly the transverse view), reveals the parabola originating in the bottom portion of the HMA layer and extending downward. Catalyst for the anomaly was not identified. The dashed vertical line was added as an attempt to document the paint mark on the surface.

Figure 5: GPR Anomaly Identified at Station 3+81 – Section 4669



Figure 6: Core Cut at Station 3+81 – Section 4669

Figure 7 illustrates the GPR trace for an anomaly identified BWP at Station 4+73. Similar to the anomaly observed at Station 2+46, a parabola indicated something just below the new HMA layer extending downward toward the CSM layer. Figure 8 is a photo of the core cut at Station 4+73 and shows a crack beginning just below the new HMA layer extending downward through the CSM layer.

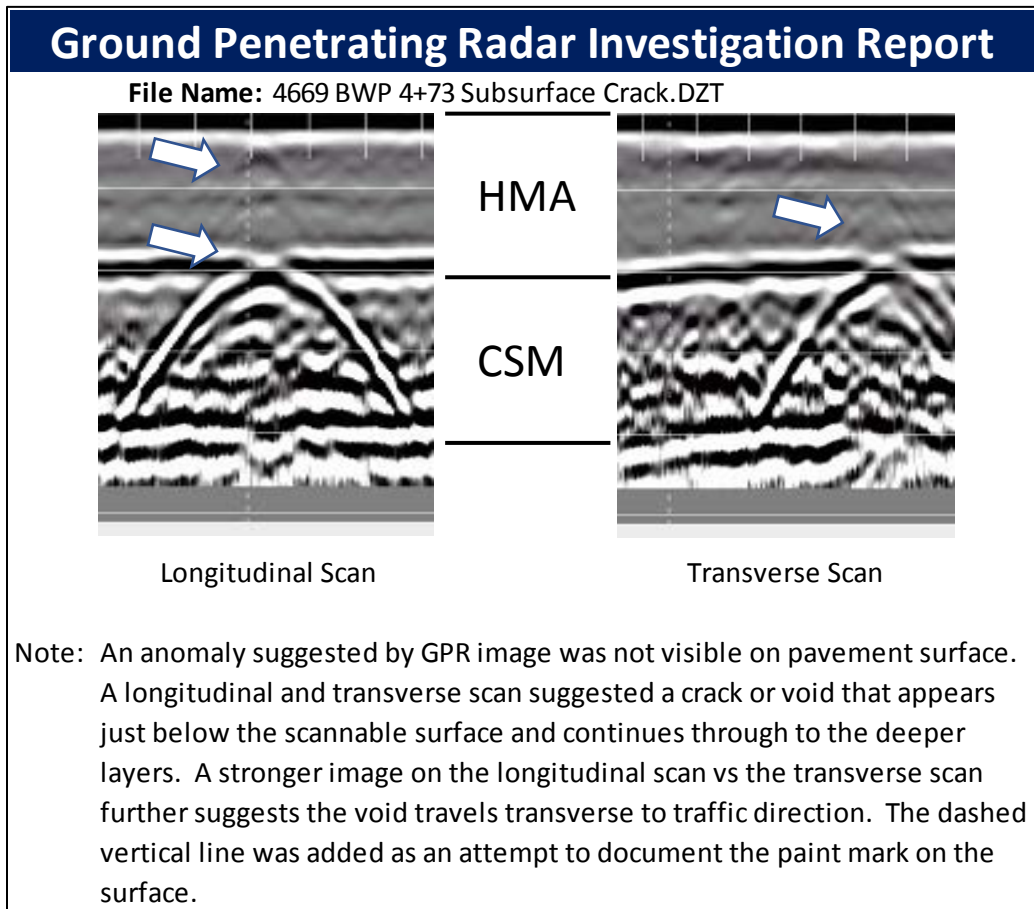
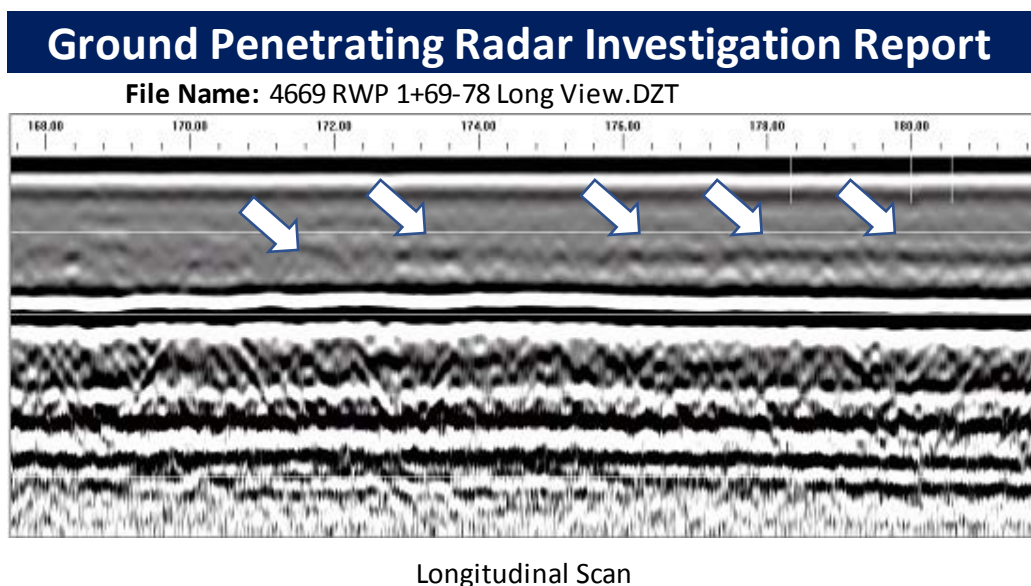


Figure 7: GPR Anomaly Identified at Station 4+73 – Section 4669



Figure 8: Core Cut at Station 4+73 – Section 4669

Figure 9 illustrates an anomaly longitudinally within the RWP between stations 1+68 and 1+78 highlighted by the white arrows superimposed onto the figure. The anomaly observed within Figure 9 is a darker line (in relation) approximately 2 to 3 in above the bottom of the HMA layer which is shown as the black/white/black sequence at approximately the half way point vertically within the trace. This anomaly suggests a contrast in the dielectric constant between two materials that drives the strength (brightness) of the reflection. Figure 10 illustrates the GPR traces transversely at Stations 1+65, 1+69 and 1+78. As shown within Figure 10, anomalies were observed at Stations 1+69 and 1+78. Figure 11 illustrates the cores cut at Stations 1+69 and 1+78. Cracks below the new HMA overlay of varying depths were found at these locations. Therefore, the contrast in the dielectric constant was most likely caused by the air of the crack versus the intact HMA above the crack.

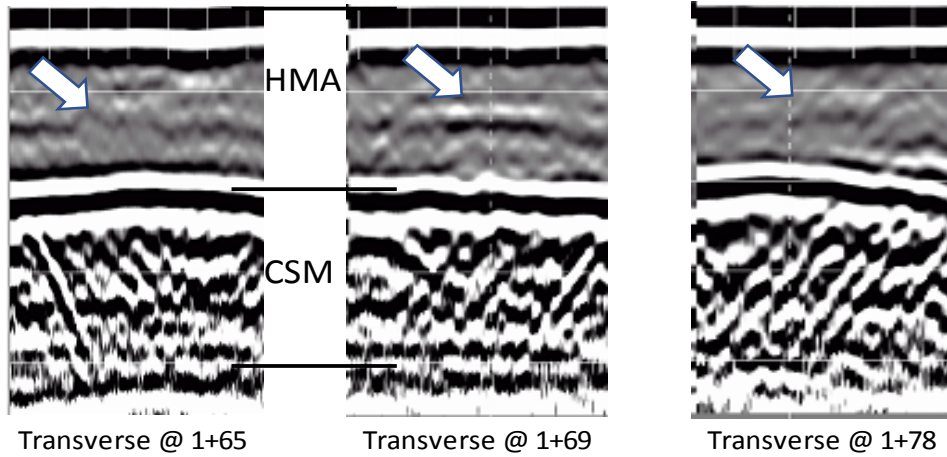


Note: An anomaly in the right wheel path seemed to continue for several feet. This can sometimes indicate you are scanning directly above and in the same direction as the object in question. Cores were taken at 1+78, 1+69, and 1+65 to investigate and possibly predict a start and stop point. It is the contrast between the dielectric constant of the two materials that drives the strength (brightness) of a reflection. Because of the low dielectric of air, a phase inversion, or flip-flopping of the polarity sequence from white/black/white to black/white/black can occur.

Figure 9: GPR Anomaly in the Longitudinal Direction Between Stations 1+68 and 1+78 – Section 4669

Ground Penetrating Radar Investigation Report

File Name: 4669 RWP 1+65-69-78 Trans View.DZT



Note: Companion Transverse Scans were performed at 1+78, 1+69, and 1+65 to further pin-point the presence and position of the observed anomaly. Voids were observed in the 1+78 and 1+69 cores.

Figure 10: GPR Anomaly in the Transverse Direction at Stations 1+65, 1+69, and 1+78 – Section 4669



Figure 11: Cores Cut at Stations 1+69 and 1+78 – Section 4669

Summary

In summary, BCD was afforded a unique opportunity at Site 4669 near Woodville, Mississippi. This unique opportunity existed because, first, the pavement had been recently rehabilitated with a mill and overlay so very few distresses were visible at the pavement surface. Secondly, because of equipment issues, BCD was able to obtain GPR traces and bring these traces back to evaluate prior to sampling the pavement section. Finally, anomalies in the GPR traces were cored at the time of field sampling to determine the cause of the anomalies. As shown in the above discussion, BCD was able to identify the cause of GPR trace anomalies in most every instance. The importance of this observation is that none of the distresses were observed at the pavement surface and would not have been found without the GPR traces.

Subsurface Anomalies within Full 500-ft GPR Trace Evaluations

One of the objectives of this study was to evaluate the potential of the GPR to identify pavement distresses (or other pavement issues) below the pavement surface that was not visible. Specifically, knowing distresses such as moisture damage (stripping), cracks which have not propagated to the pavement surface, cracking in CSM layers, fatigue in CSM, etc. would be important during the M&R design process. The following describes anomalies found within the GPR traces that potentially identify subsurface distresses. These discussions of potential subsurface distresses only present a sampling of the anomalies found for each category.

Stripping in HMA

The occurrence of potential stripping within the HMA was observed within Section 3163. Figure 12 illustrates the RWP and right pavement edge (RPE) traces within Section 3163 near station 3+16. Superimposed onto the left side of the traces are the typical pavement structure for the section. The top trace shows that the HMA for the RWP (top trace) is relatively consistent in color and shade. However, within the RPE trace (lower trace) there is a distinguishable darker line (highlighted by the white arrows within the figure) several inches above the interface between the HMA and CSM layers (white/black/white lines at bottom of HMA). This darker line in the RPE trace also has some characteristics of an interface in that faint white lines can be observed just above and below the darker line. The existence of this faint interface likely suggests a change in material properties that could indicate stripping or possibly delamination between HMA layers. A solid vertical white line has been superimposed onto the RPE trace to signify a potential boundary in which the anomaly ends. Stripping was observed within some cores cut from Section 3163.

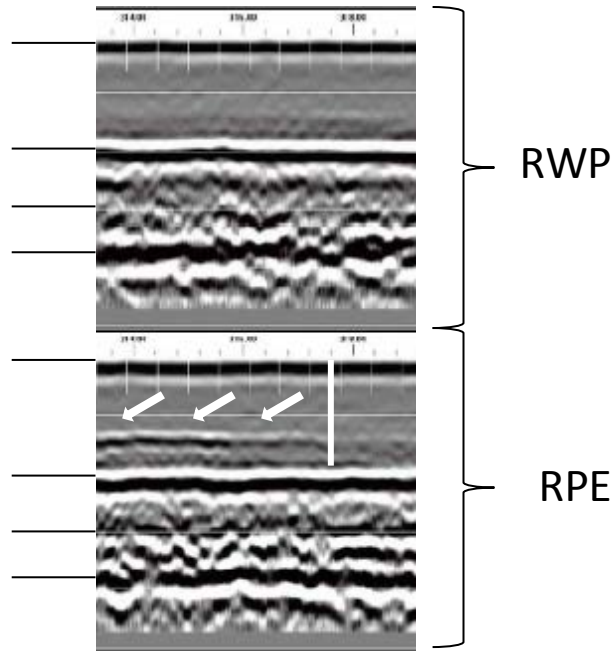


Figure 12: RWP and RPE Traces from Section 3163 near Station 3+16

Another instance of potential stripping was observed in Section 4834. Figure 13 illustrates the BWP trace for Section 4834 at approximately station 0+19. This figure shows a shadowing above the HMA/CSM interface (highlighted by the white arrow). This anomaly is an isolated area within the trace and may indicate stripping. However, cores cut in other areas of Section 4834 showed very little stripping.

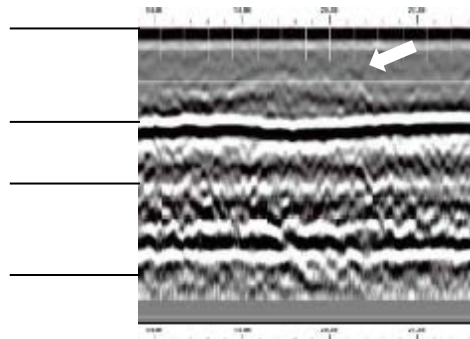


Figure 13: BWP Trace from Section 4834 near Station 0+19

Traces from Section 4864 also had anomalies within the HMA that could potentially be stripping. Figure 14 illustrates the RWP trace of section 4864 near station 0+45. As shown in the figure, there are some anomalies above the HMA/CSM interface and within the HMA. The anomalies appear as small wavy lines within the HMA. These anomalies may be indicating stripping. Stripping was observed within lower HMA layers for section 4864.

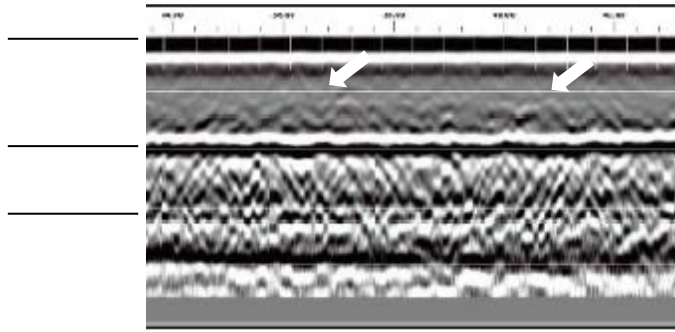


Figure 14: RWP Trace from Section 4864 near Station 0+45

Similar to Figure 12, Figure 15 shows a characteristic dark line within the HMA layer which may indicate stripping or possibly delamination for section 5244. The trace within Figure 14 is from the left wheel path (LWP) near station 0+52. As shown in Figure 15, this dark line is not visible on the left side of the figure which may indicate a boundary between stripped and non-stripped HMA. Stripping was observed within the lower HMA layers at a number of core locations within this section.

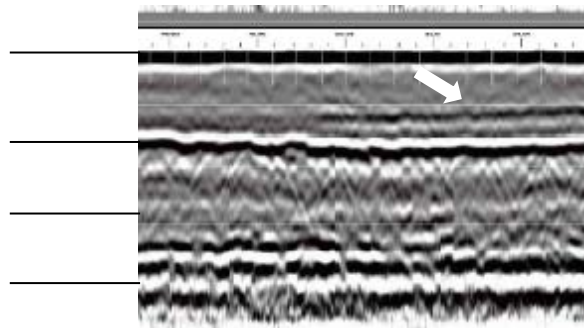


Figure 15: LWP Trace from Section 5244 near Station 0+52

Also, within section 5244, Figure 16 shows a layering within the HMA layer that could indicate stripping. This trace is from the left pavement edge (LPE) near station 2+24. Because this trace is at the LPE, it is near the longitudinal joint between lanes. The layering effect shown in the figure may be the GPR identifying the offset of longitudinal joints as the HMA structure was built.

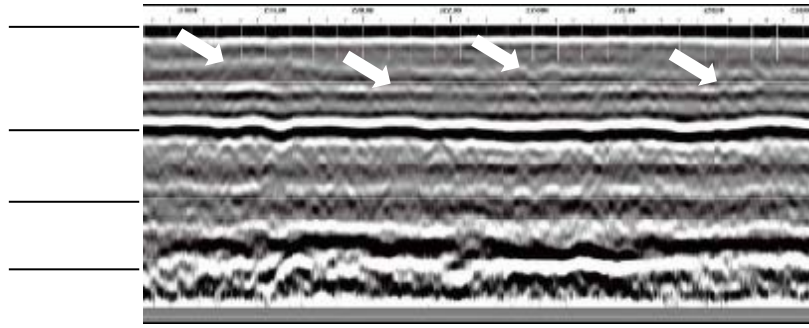


Figure 16: LPE Trace from Section 5244 near Station 2+24

The final example of possible stripping is from Section 5230 near station 3+00. Figure 17 illustrates the characteristic darker line above the HMA/CSM interface that was seen in other traces. For this particular location, cores were obtained for testing during SS No. 263. As illustrated within Figure 17, the darker line is a couple inches above the interface. The core shown in Figure 17 was cut within a couple feet of the location of the GPR trace. Two conditions are depicted within the picture of the core. First, stripping is observed a couple inches from the bottom of the HMA layer. Secondly, the layer in which the stripping occurred has also delaminated from the overlying layer.

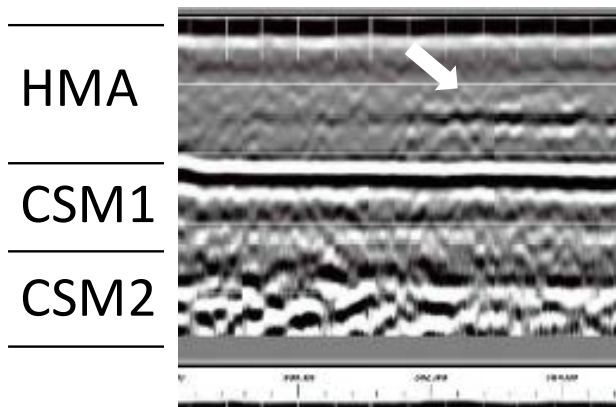


Figure 17: BWP Trace from Section 5230 near Station 3+00

Based upon the evaluation of the full 500-ft GPR traces for the 16 sections, stripping may be a difficult distress to observe. Only future coring of the layers will verify whether the GPR is successful in identifying the occurrence of stripping. One observation from Figure 17 is that the characteristic dark line may indicate the combination of stripping and delamination.

Crack at Bottom of HMA Layer

Cracking within the HMA layer was observed throughout the layer. Sometimes the crack appeared to initiate near the surface, sometimes the cracks appeared to initiate mid-level and some appeared to only be near the bottom of the layer. This section only describes HMA cracks that appeared to be limited to the bottom of the HMA layer.

Figure 18 illustrates the occurrence of cracks that appear to be limited to the bottom portion of the HMA layer in Section 5230. The top trace within Figure 18 is the LWP trace while the bottom is the BWP trace. Within both of these traces, an anomaly within the lower portion of the asphalt layer can be observed. Interestingly, the two anomalies have different appearances. Within the LWP trace, the anomaly is a large parabola, while in the lower trace the anomaly is a smaller parabola. It's unclear why the parabolas are different; however, one explanation could be the width of the cracks are different.

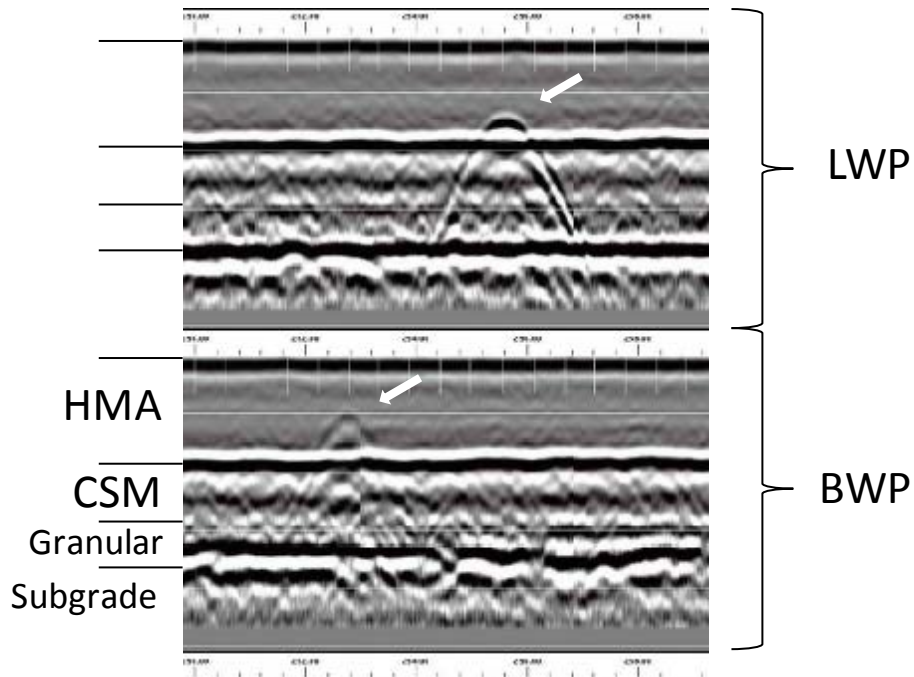


Figure 18: LWP and BWP Traces from Section 5230 near Station 2+54

Another instance of a potential crack within the lower part of the HMA layer is from section 4784. Figure 19 illustrates this potential crack. This trace is from BWP near station 1+98. As shown in the figure, the crack appears to be just a couple inches above the HMA/CSM interface.

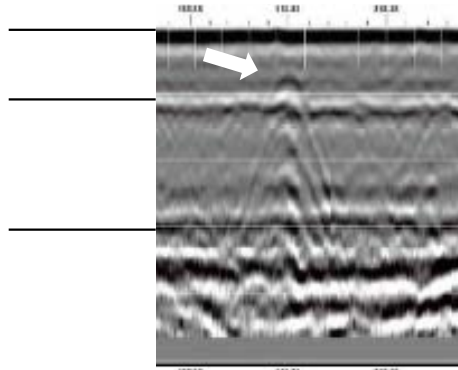


Figure 19: BWP Trace from Section 4784 near Station 1+98

Figure 20 illustrates another potential crack that is near the bottom of the HMA layer. This trace is from the LPE near station 1+02 within Section 4834. This particular anomaly appears to be right at or just above the HMA/CSM interface.

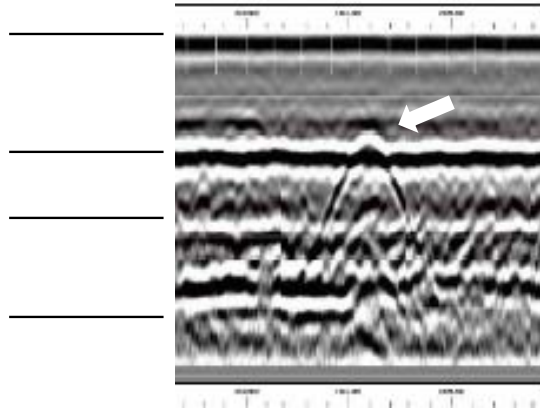


Figure 20: LPE Trace from Section 4834 near Station 1+02

A final example of a crack within the HMA layer that appears to be within the bottom portion of the layer is illustrated in Figure 21. This trace is from section 5210 near station 0+34 and represents the LPE. The small anomaly is just above the HMA/CSM interface. This anomaly is a little different than the others presented within this section. The other anomalies presented in this section had the characteristic parabola. Figure 21 does not show the parabola; rather, the anomaly is a convex shape that is isolated to the anomaly. Interestingly, there is a color change from black to white within the anomaly. Because of the color change, the anomaly could be a small void at the bottom of the layer or some type of foreign material.

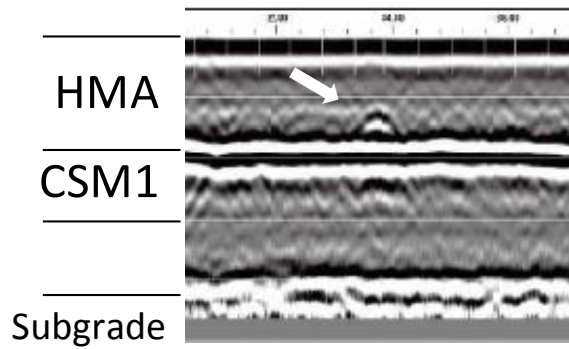


Figure 21: LPE Trace from Section 5210 near Station 0+34

Based upon the presentation of these anomalies that appear to be cracks near the bottom of the HMA layer, it would be difficult to state how the cracks initiated. If in fact these anomalies are cracks, initiation of the crack could in some instances be from fatigue and in other instances could be cracks reflected upward from the CSM layer(s). For instance, the large anomaly within the LWP trace of Figure 18 could suggest a much wider crack than the smaller parabola within Figure 21. The indication (suggestion) of a wider crack may be because the CSM layer has cracked and is beginning to reflect upward.

Crack Mid-Depth Within HMA Layer

In some instances, it appeared that the tops of cracks (anomalies) were within the middle of the HMA layer. These instances are based upon the top of the parabolas being about mid-level within the HMA layer. Figure 22 illustrates an anomaly that appears to begin at approximately mid-depth of the HMA layer. This trace is from the RWP near station 0+92 of Section 2580. As shown in the figure, a parabola exists within the middle portion of the HMA layer. The existence of this parabola suggests that a crack has potentially initiated mid-depth within the HMA layer, the crack existed prior to a mill and overlay, or reflected from the underlying CSM.

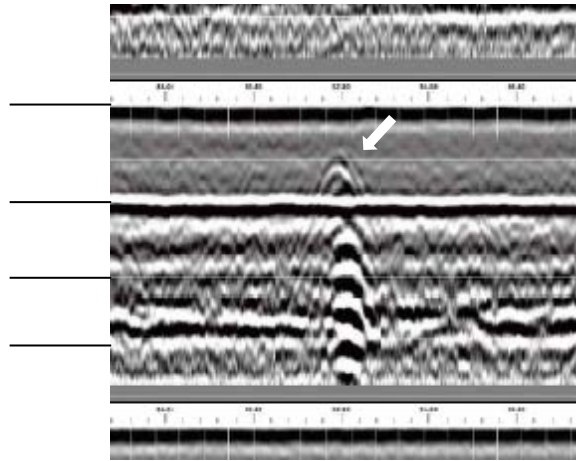


Figure 22: RWP Trace from Section 2580 near Station 0+92

Another instance of a potential mid-level crack was observed within Section 3163 near station 0+12. Figure 23 illustrates the LWP trace and the characteristic parabola indicating the crack. Interestingly, the interface between the HMA and CSM is very consistent, suggesting the crack (anomaly) is not reflected from the CSM. Also, the parabola does not appear to extend into the CSM layer.

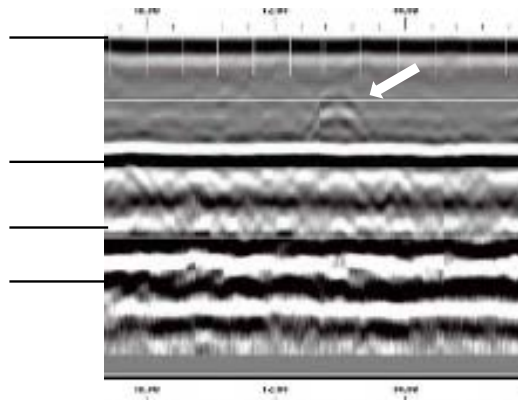


Figure 23: LWP Trace from Section 3163 near Station 0+12

Figure 24 illustrates a trace of the LWP near station 3+34 for section 4588. This figure shows a parabola that starts at approximately mid-depth of the HMA layer. The existence of these mid-layer anomalies is interesting. Three possibilities for these types of anomalies have been provided, if in fact they are cracks. Namely, these could be cracks that initiated mid-layer, reflected upwards from the CSM or existed prior a mill and overlay. The only method of determining the cause of these anomalies will be to core the pavements.

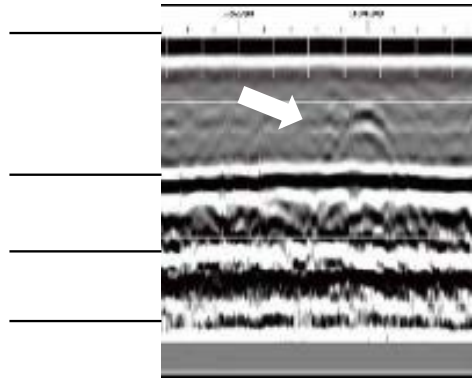


Figure 24: LWP Trace from Section 4588 near Station 3+34

Crack Within CSM Layer

Another common type of anomaly observed within the five full 500-ft traces was potentially a crack within the CSM layer. These instances were individual parabolas showing at the top of the CSM layer. A representative trace showing potential cracks within the CSM layer is illustrated within Figure 25. This trace is from the LWP of section 3163 near station 2+16. As shown by the white arrows within this trace, a number of potential cracks are illustrated. In addition to the parabola that begins at the interface between the CSM and HMA layers, one characteristic of these potential cracks within the CSM layer that is common is the distinct small concave shape at the interface. This characteristic was observed on many of the potential CSM layer cracks.

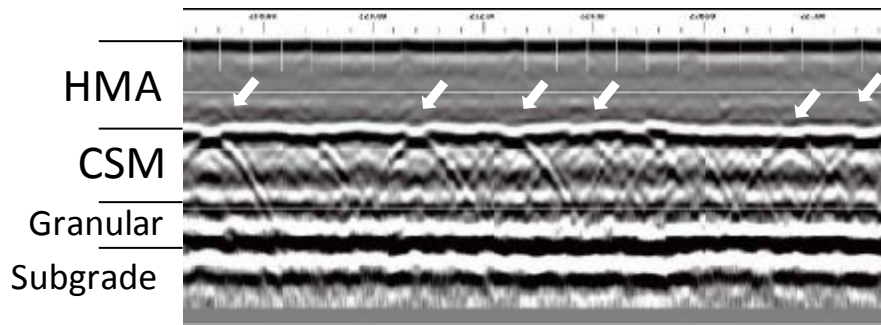


Figure 25: LWP Trace from Section 3163 near Station 2+16

Recall back to Figures 7 and 8 from section 4669. Figure 7 showed the GPR trace for the pavement anomaly that caused the core to be cut. This GPR trace also showed the characteristic concave shape at the interface of the CSM and HMA layers. Figure 8 showed that

a crack did exist in the CSM layer. Therefore, this small concave shape at the interface of the HMA and CSM layers may be an indication of a crack at the surface of the CSM layer.

Figure 26 illustrates another anomaly that likely shows a crack within the CSM layer. This trace is from the LPE of Section 4782 near station 2+86. This figure again shows the characteristic concave shape at the interface between the CSM and HMA layers. However, this trace also shows an anomaly above this concave shape that could suggest that the crack within the CSM layer has propagated upwards into the HMA layer (above the left white arrow). As discussed elsewhere in this report, it has been hypothesized that cracks reflected into the overlying HMA layer may not be directly above the CSM crack. Figure 26 suggests this may again be the case.

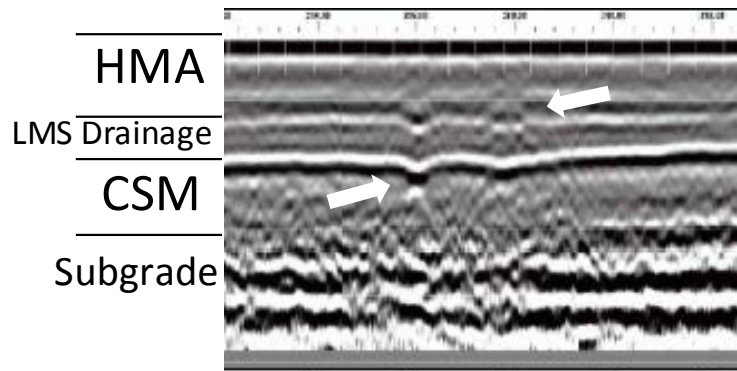


Figure 26: LPE Trace from Section 4782 near Station 2+86

Another instance of potential cracking within the CSM layer is illustrated within Figure 27. This figure shows the RPE trace from section 4784 near station 0+50. This figure shows two distinct parabolas, one at the top of the CSM layer and one at approximately the midpoint of the CSM layer. The occurrence of the anomaly in the middle of the CSM layer is interesting as only a single layer of CSM material was within the pavement structure. It is possible that if the anomaly is not a crack, it could be a large aggregate particle or some foreign material within the layer.

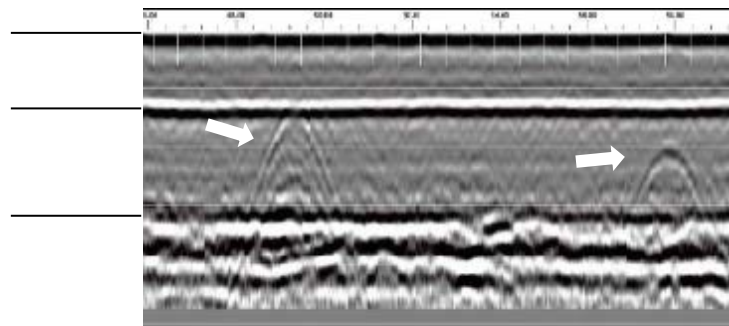


Figure 27: RPE Trace from Section 4784 near Station 0+50

Figure 28 illustrates the occurrence of an anomaly at the top of the CSM layer that appears to be a crack within the CSM layer. Figure 28 is the LPE trace from section 5210 near station 0+58. Similar to other traces indicating a crack within the CSM layer, a characteristic concave shape is located at the top of the parabola.

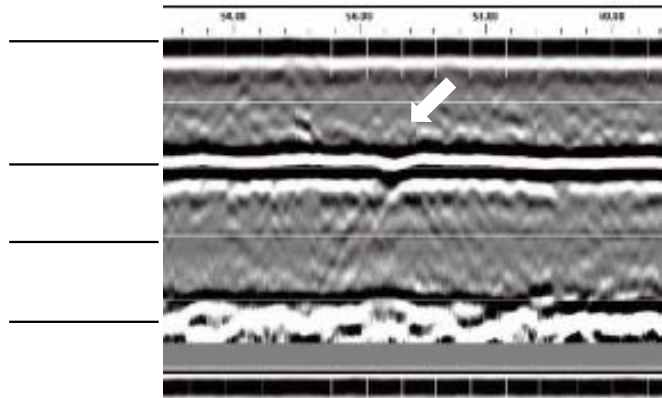


Figure 28: LPE Trace from Section 5210 near Station 0+58

A large number of traces appeared to indicate cracks within the CSM layer. Typically, a parabola existed at the interface of the HMA and CSM layer. One characteristic that did seem to accompany these parabolas was the existence of a small concave distortion of the interface.

Fatigue Cracking Within CSM Layer

Fatigue cracking within a CSM layer is a subsurface distress that would be vitally important when conducting a M&R design. A CSM layer that has fatigued will not have the same structural capacity as a CSM layer that is intact. Therefore, the areal extent of CSM fatigue would be important. Figure 29 illustrates a circumstance in which the GPR trace suggests fatigue cracking within the CSM layer. This trace is from the RWP of section 2580 near station 1+34. As shown on the figure, this section included two layers of CSM below the HMA layer. Based upon evaluation of all 16 sections included within Table 1, the characteristic that suggests the potential for fatigue within the CSM layer is the clarity of the interface, or the changes in clarity, of the interface between the CSM and underlying layer. As shown within Figure 29, the interface between the second CSM layer (CSM2) and subgrade is clear and distinctive on the left side of the figure. On the right side of the figure, the clarity of the interface is much less. A white vertical line was superimposed onto Figure 29 to indicate a potential boundary between an area in which the CSM is fatigued and the area which is not. Based on the figure, the first layer of CSM (CSM1) seems to be intact, while the boundary seems to be for the CSM2; however, without coring the specific layer and/or boundary cannot be verified.

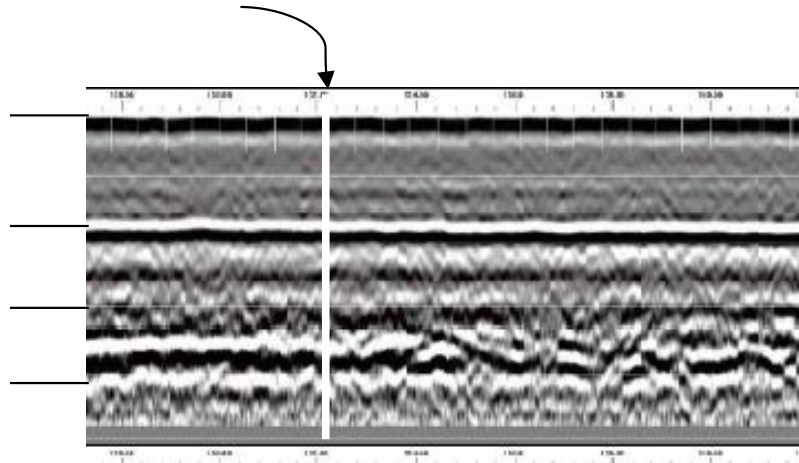


Figure 29: RWP Trace from Section 2580 near Station 1+34

Figure 30 illustrates another trace that suggests fatigue within a CSM layer. This figure shows the trace for the RWP of section 4588 near station 3+34. Figure 30 is different from Figure 29 in that the interface between the two CSM layers is reasonably consistent; however, the CSM1 material appears to be inconsistent on the right side of the superimposed boundary line. This could suggest that CSM1 is fatigued.

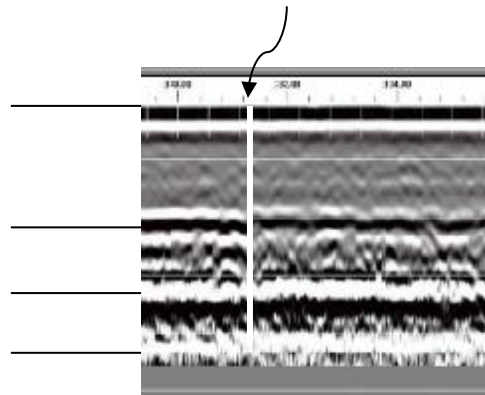


Figure 30: RWP Trace from Section 4588 near Station 3+34

Another occurrence of potential CSM fatigue is illustrated within Figure 31. This trace is from the RWP of section 5244 near station 1+00. The pavement structure within section 5244 only included a single layer of CSM. As shown in the figure, the potential occurrence of fatigue within the CSM layer is different in appearance within Figure 31 than in Figures 29 and 30.

Within Figure 31, a series of parabolas beginning at the CSM/HMA interface is the characteristic that suggests fatigue cracking. The large number of parabolas distort the interface between the CSM and HMA layers.

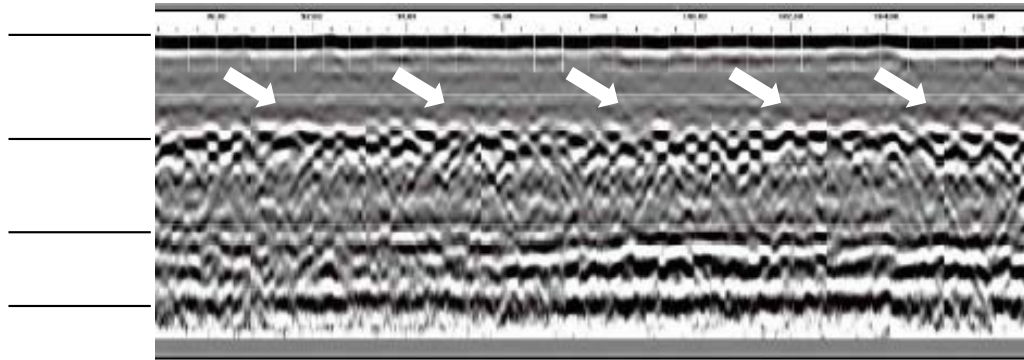


Figure 31: RWP Trace from Section 5244 near Station 1+00

The final presented occurrence of possible fatigue within the CSM layer is illustrated within Figure 32. These traces show the RWP and RPE of section 5249 near station 3+50. As shown in the figure, the interface between the CSM and subgrade is distinct for the RPE, while within the RWP trace the interface is broken in areas. This may suggest CSM fatigue within the RWP.

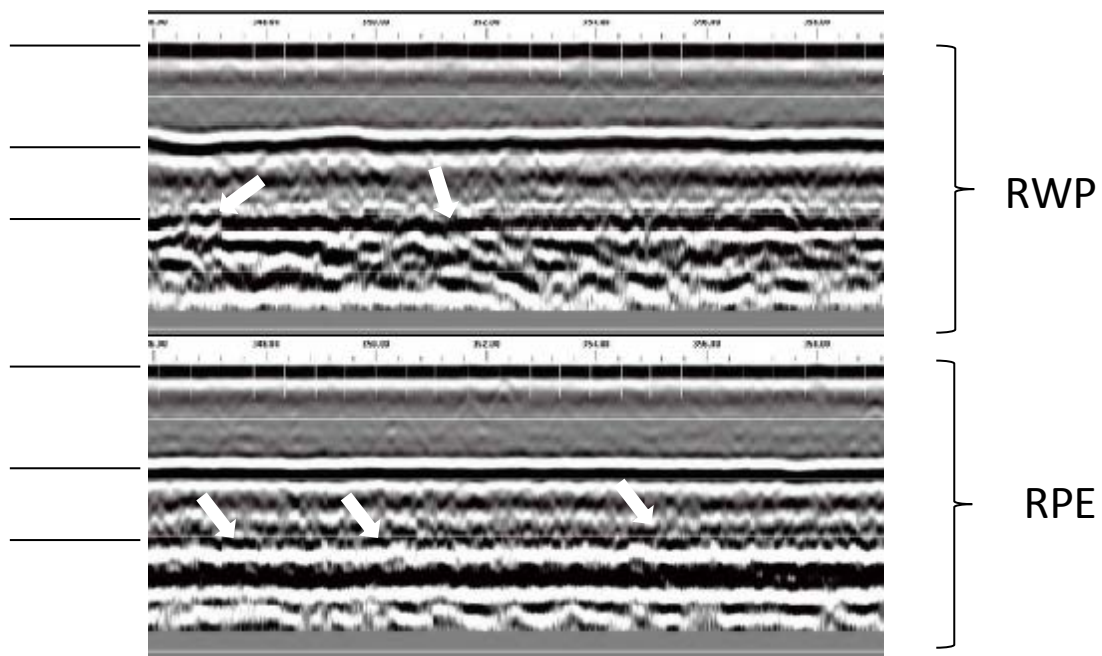


Figure 32: RWP and RPE Traces from Section 5249 near Station 3+50

Fatigue within the CSM layer(s) would be important within a M & R design. Successful interpretation of GPR traces to identify fatigue within CSM layers would be a major benefit. However, the only method to verify the existence of the fatigue would be coring.

Interesting Observations from Five Full 500-ft Traces

While evaluating the five full 500-ft traces for the 16 sections, a number of observations were categorized as interesting. Though some may or may not specifically affect a M&R design, they are presented to illustrate the potential of the GPR to identify potential issues within the pavement. The first interesting observation is from the RWP near station 0+56 within section 4588, which is shown in Figure 33. As shown in the figure, the thickness of the HMA layer changes (white arrow). Based upon the trace, the thickness of the HMA changed approximately 1 inch.

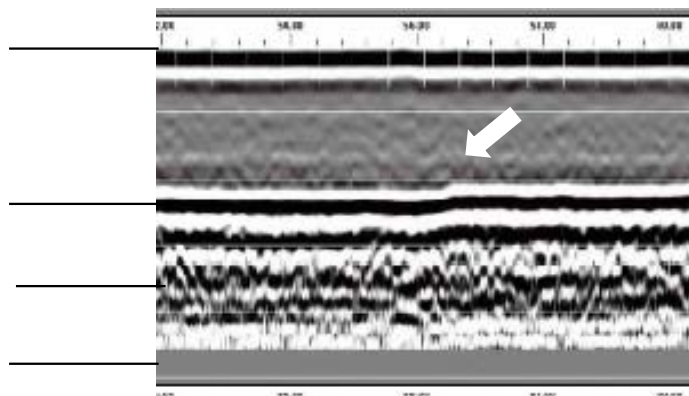


Figure 33: RWP Trace from Section 4588 near Station 0+56

Another interesting observation comes from section 4782. A transverse crack existed near station 3+30 that extended across the entire lane. As shown within Figure 34, which shows all five traces near 3+30, the transverse crack was identified by the GPR across the entire lane width (white arrows). Another interesting observation about the traces is that there are the characteristic concave shapes at the HMA/CSM interface that was described previously (white circle). This transverse crack was selected in the field for coring. Figure 35 presents photos of the pavement surface, the transverse crack, the full depth core, and the surface of the CSM within the core hole. As shown within Figure 35, a crack existed within the CSM layer (which has been hypothesized for the characteristic concave shape) and the crack extended through the entire HMA layer. This may suggest that when the characteristic concave shape is located at the top of the CSM layer and the crack is visible at the surface, the crack is full depth within both the CSM and HMA.

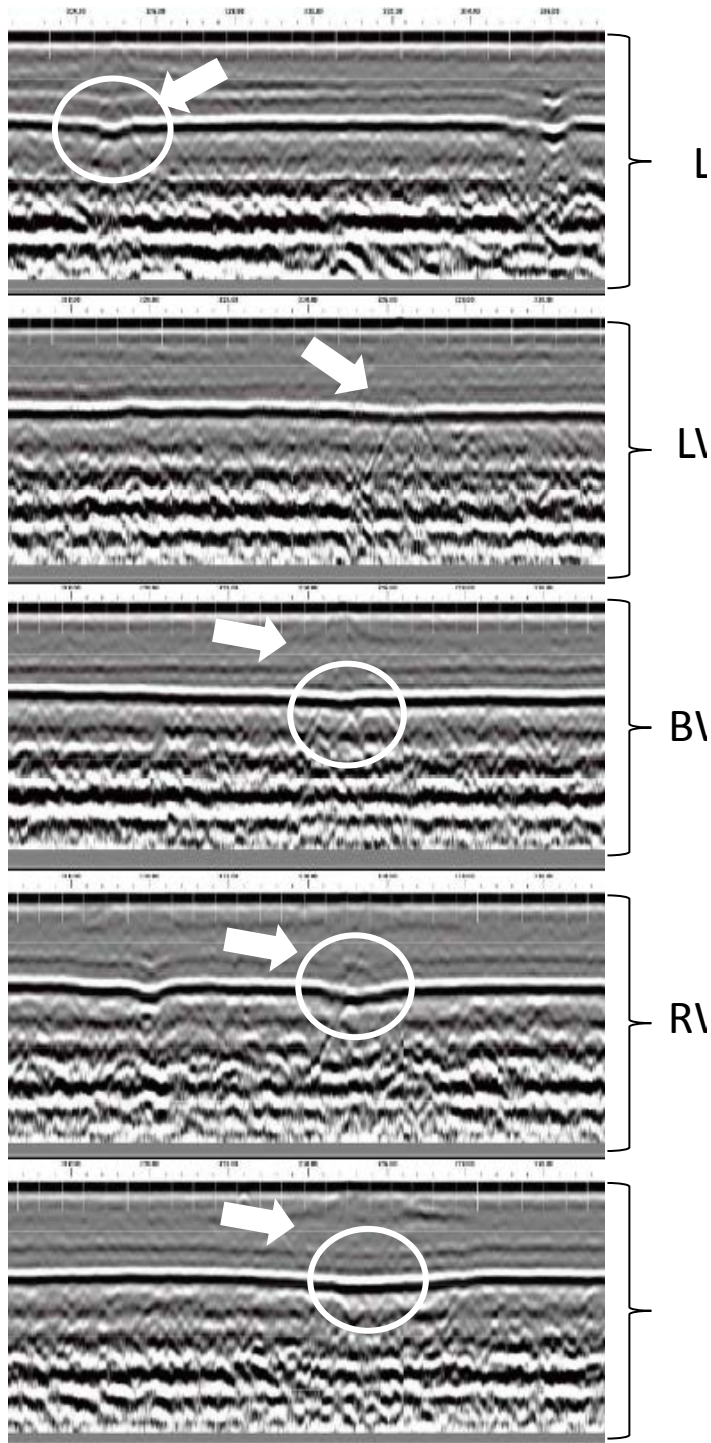


Figure 34: Five Traces from Section 4782 near Station 3+30

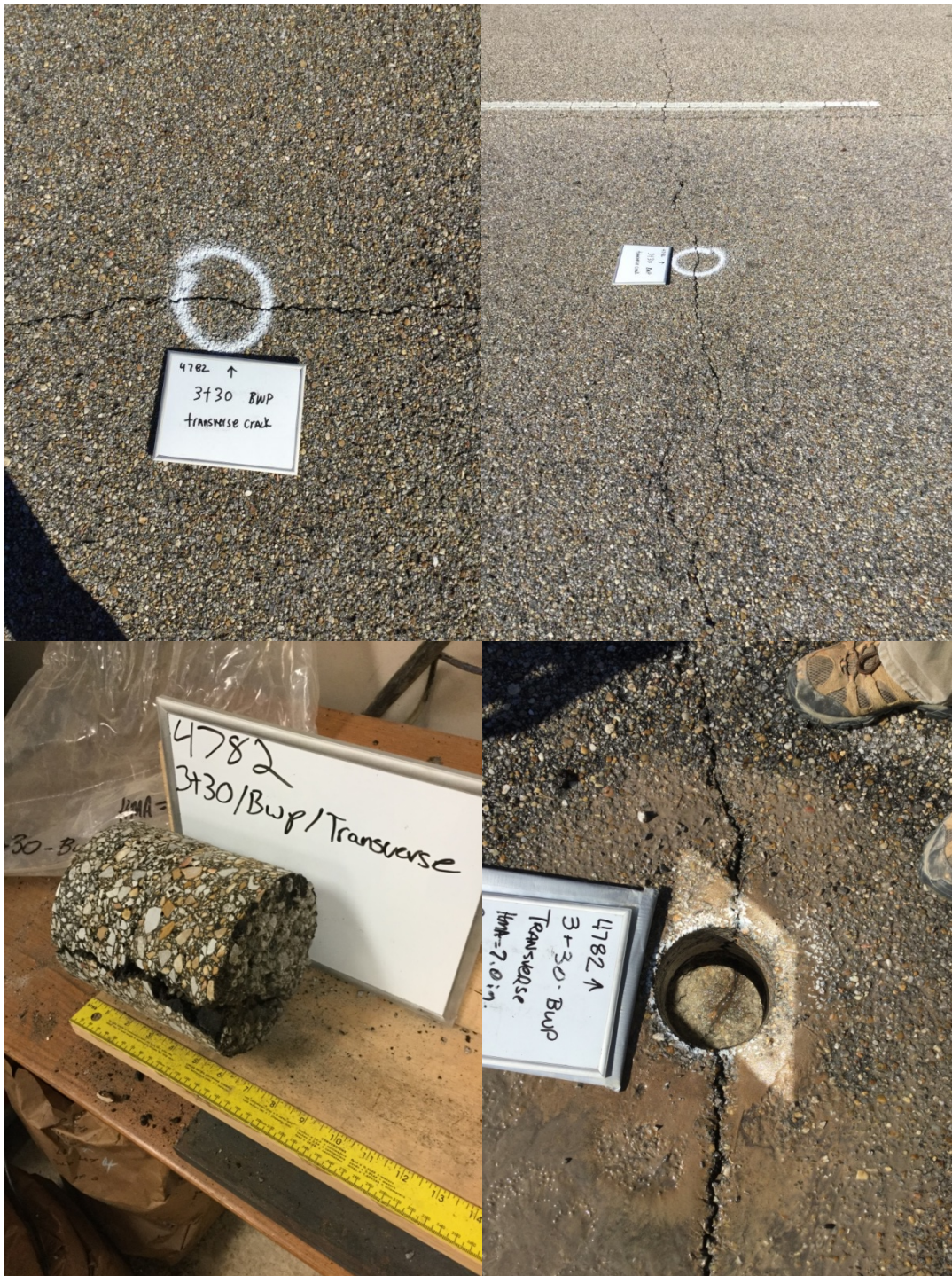


Figure 35: Photos of Pavement Surface and CSM Layer near Station 3+30 in Section 4782

Section 4782 provided another interesting observation from the GPR traces. Figure 36 presents a BWP trace near station 3+35. As shown on the left side of the figure, an anomaly exists within what is believed to be the limestone (LMS) drainage layer. The top of the anomaly (parabola) appears to be right at the interface between the LMS drainage layer and HMA. It is

unclear whether this is potentially a crack within the underlying CSM that is propagating upward through the LMS Drainage layer, a discontinuity within the LMS drainage layer or some foreign matter. Intuitively, it would not be a crack propagating through the LMS Drainage layer into the HMA; therefore, the likely cause is a discontinuity or foreign material within the LMS Drainage layer. Secondly, there is a dark horizontal line that begins about a third of the distance from the left of the trace that extends to the right edge of the trace. At about the half-way point of the trace, the dark horizontal line goes downward then comes back up. When it begins, this dark horizontal line would be near the interface between the HMA and LMS drainage layer. It is unclear why this dark horizontal line is within part of the trace and not the other. It is also unclear why the dark horizontal line would drop and then rise within the trace. The larger white arrows oriented upwards show the characteristic small concave shape at the interface of the HMA and LMS Drainage layer which may be indicating cracks within the CSM layer.

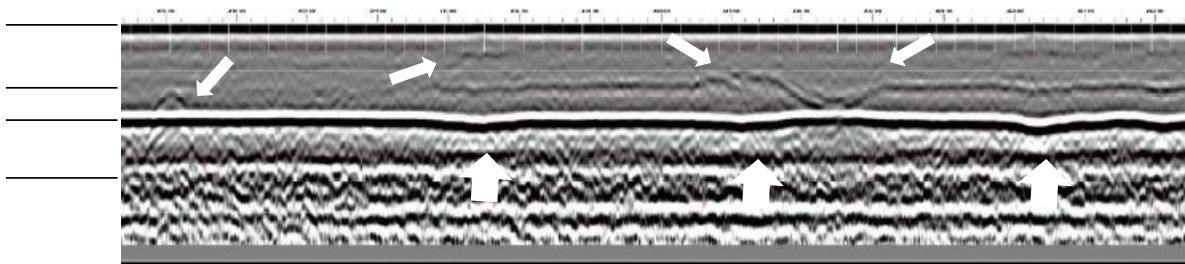


Figure 36: BWP Trace from Section 4782 near Station 3+35

Section 4834 also provided a unique trace. Figure 367 presents a trace from the RPE near station 0+70. As shown within this figure, the interface between the HMA and CSM has an isolated convex shape. It is also interesting that the interface between CSM2 and the subgrade changes (lower white arrow) almost directly below the convex shape. The change in this interface may indicate distress within one or both CSM layers.

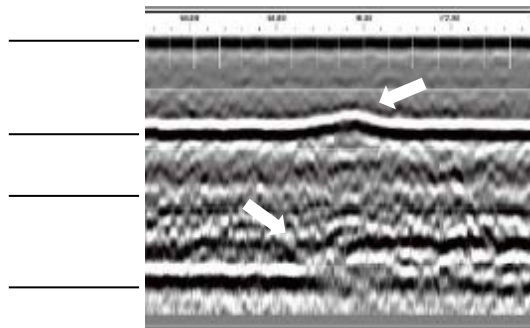


Figure 37: RPE Trace from Section 4834 near Station 0+70

Figure 38 presents a trace from the LWP of section 5210 near station 0+24. This trace shows two parabolas (anomalies). One parabola is within the HMA layer while the other parabola is within the CSM1 layer. The interesting part of this trace is that the two parabolas appear to be offset by a short distance. During the field work within SS No. 263, there were a number of instances where a transverse crack existed within the HMA surface. Based upon the appearance of the transverse crack in the field, it was assumed that the transverse crack had reflected from a crack within the CSM layer; however, after coring a crack was not observed within the CSM layer. The trace within Figure 38 potentially suggests that the reflected crack within the HMA may not always be directly above the crack within the CSM layer.

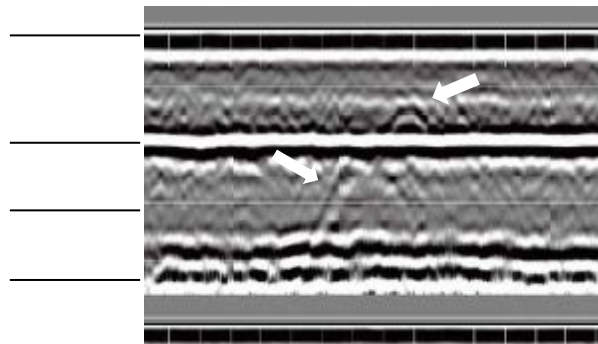


Figure 38: LWP Trace from Section 5210 near Station 0+24

Figure 39 presents a trace from section 5230 near station 2+96. This figure illustrates the LPE and LWP traces at the location. Based on the figure, the interface between the two CSM layers was very inconsistent within the LPE trace. The LWP trace also shows this inconsistency within the CSM layers; however, it is not as distinct. It is unclear why the interface between the two CSM layers would be so inconsistent. One possibility is that within this area, the construction of the CSM layers was inconsistent. On the LWP trace, a white arrow within the HMA layer shows a small area having differing/alternating shades of gray. This area may indicate a small area of stripping.

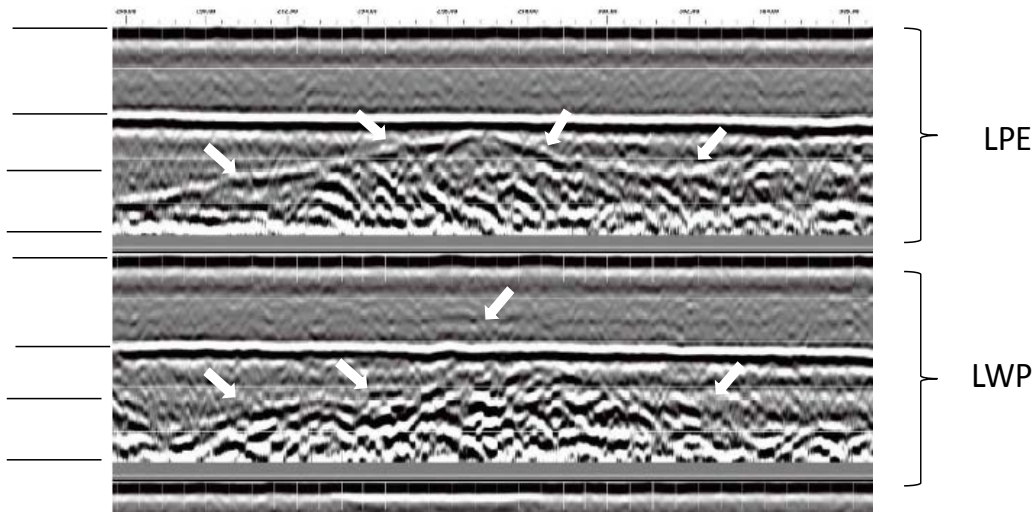


Figure 39: LPE and LWP Traces from Section 5230 near Station 2+96

The final interesting observation presented herein is presented within Figure 40. This figure shows the RPE trace from Section 5249 near station 1+25. As shown in the figure, the interface between the HMA and CSM is very inconsistent. It's unclear whether subsurface distresses are distorting the interface or whether the HMA layer thickness is variable in this area.

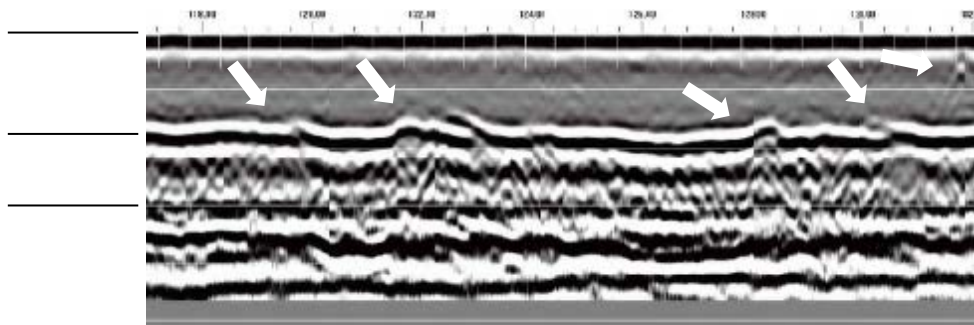


Figure 40: RPE Trace from Section 5249 near Station 1+25

A number of interesting observations from the GPR traces were provided. The offset parabolas within Figure 38 appear to provide some explanation for the reason that some CSM cracks were not observed when they were expected. The issues highlighted within Figures 39 and 39 do suggest something happening below the HMA layer that would need further investigation.

Summary

This section of the report presented GPR traces that indicated potential subsurface distresses/issues. While evaluating the full length GPR traces, several trace characteristics were identified as indicating subsurface distresses/issues. Related to stripping (moisture damage)

within the HMA layers, two characteristics were found. First, a darker line within the HMA is believed to be related to stripping. This was illustrated in Figures 12, 15 and 17. This darker line may also be related to the combination of stripping and delamination based upon Figure 16. In addition to the darker line, several areas of various shades of gray and small lines may indicate stripping as shown in Figures 13 and 14.

Parabolas within a GPR trace are believed to generally indicate subsurface cracks. Based upon the various traces evaluated, parabolas were identified near the bottom of the HMA layer as well as the middle of the HMA layer. These parabolas were also found within the CSM layers. Another characteristic that may be related to cracks at the top of CSM layers is a small concave shape at the interface of the HMA and CSM layer.

Identification of potential fatigue within the CSM layer(s) was based upon two conditions. First a series of close parabolas with the peaks being at the HMA/CSM interface as shown in Figure 31 may indicate fatigue. A second condition was the change in clarity of the interface of the CSM and underlying layer.

Each of the above described potential subsurface distress could potentially affect the design of M & R strategies for existing roadways. Therefore, the identification of the distresses is important. If the GPR can help identify these distresses, it would be a benefit to MDOT.

GPR Traces of Visible Distresses

At each of the 64 test sections evaluated and sampled during SS NO. 263, specific surface distresses were selected from within the 500-ft section for further evaluation. Both typical and nontypical surface distresses were cored in an effort to identify the mechanism that initiated each of the distresses. Typically, between four and ten of the surface distresses were selected for further evaluation depending upon the condition of the pavement. Surface cracks visible at the pavement surface can be categorized into three general categories, including: longitudinal cracks, transverse cracks and fatigue cracks.

It should be stated that the term fatigue crack is based upon the definition provided within the *Distress Identification Manual for the Long-Term Pavement Performance Project (2)*. This document states that fatigue cracking occurs within wheel paths due to repeated traffic loadings. Historically, this definition has been believed to be cracks that initiate at the bottom of the HMA layer.

Low severity fatigue cracking is “an area of cracks with no or only a few connecting cracks; cracks are not spalled or sealed; pumping is not evident (2).” This definition of low severity fatigue cracking is important to this document because a significant percentage of the fatigue cracks were found to not have initiated at the bottom of the HMA layer.

For each of the selected surface distresses, two GPR traces were obtained. Each of these two traces were 2- to 3-ft in length. One trace was transverse to the direction of travel and the second trace was in the longitudinal direction. Both traces were over the surface distress in an effort to determine the ability of the GPR to characterize each distress. The GPR used for this testing allowed for pinpointing a specific location on the trace for further analysis. This utility was used in the office to identify the location within each trace that the surface distress had manifested to the pavement surface.

Analysis of these visible distress GPR traces was somewhat more difficult than the full 500-ft traces. When analyzing the full 500-ft traces, changes within the trace were more obvious because the anomaly was different than the remaining part of the full-length trace. When analyzing the short traces of the specific distresses, the ability to compare the area to the full-length trace was not available. This section presents examples of the GPR traces on specific surface visible distresses for the 16 sections listed within Table 1.

For each of the GPR traces within this section, a comment is provided about the dielectric constant. As stated above, a core was cut at each of the locations discussed in this section. The dielectric constant was selected in order to provide the correct HMA thickness similar to ground-truth cores.

GPR Traces for Visible Longitudinal Cracks

Figure 41 illustrates the GPR trace for a longitudinal crack within Section 4588 near station 1+60. Black arrows shown on the figure are superimposed onto the trace to signify the location of the visible crack at the pavement surface. For longitudinal cracks, generally speaking, the GPR trace transverse to the direction of traffic would show the distress better than the longitudinal GPR trace. The transverse to traffic trace is on the right side of Figure 41, while the longitudinal trace is on the left. As shown in the figure, very little can be discerned from either the transverse or longitudinal traces related to the surface distress. Figure 42 is a collage of photographs from the location depicted by the traces within Figure 40. Photos within Figure 42 are for the pavement surface and the core obtained from the location. As shown within Figure 42, the longitudinal crack is a low severity crack which appears to have initiated at the top of the pavement surface. As shown in the lower right portion of Figure 42, the crack only extends a short distance into the HMA layer.

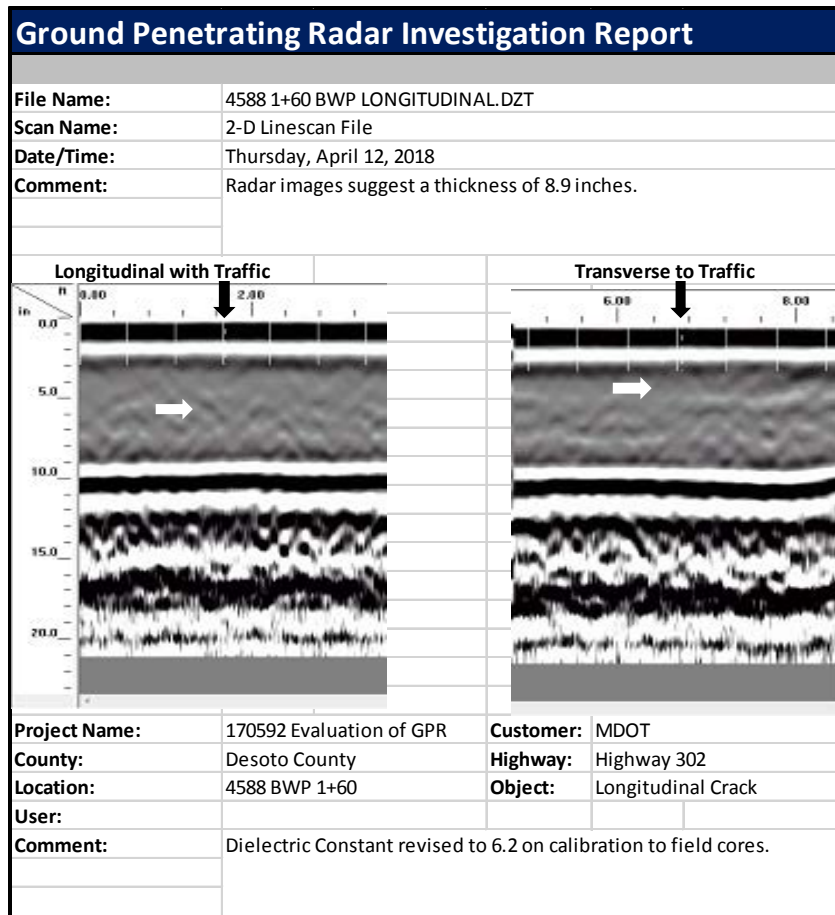


Figure 41: GPR Trace for Longitudinal Crack - Section 4588, Station 1+60

As shown in Figure 41, very little can be discerned from the traces related to the longitudinal crack that was visible at the surface of the pavement. One potential reason the GPR trace did not indicate the crack is the fact a ground coupled GPR was utilized for this testing. According to Scullion and Saarenketo (3), it can be difficult to obtain quantitative information near the pavement surface when using a ground coupled system. Figure 42 shows that the crack was low severity and did not propagate but a short distance into the pavement.



Figure 42: Pavement Surface and Core for Longitudinal Crack - Section 4588, Station 1+60

Figure 43 illustrates the longitudinal and transverse traces for a longitudinal crack within Section 4864 near station 1+00. Unlike Figure 41, the GPR traces within Figure 43 do show anomalies related to the longitudinal crack. Within the transverse trace, a characteristic parabola is shown near the top of the pavement. Within the longitudinal trace, anomalies are also shown at approximately mid-layer and near the bottom of the layer.



Figure 44: Pavement Surface and Core for Longitudinal Crack - Section 4864, Station 1+00

GPR traces for a longitudinal crack within Section 4865 near station 0+12 are illustrated within Figure 45. As shown within this figure, the transverse GPR trace shows a characteristic parabola indicating the longitudinal crack. Figure 46 illustrates the pavement surface and core obtained at this location. The photograph of the core shows that the longitudinal crack does

not extend through the entire layer of HMA. The crack extends from the surface of the pavement to just below the mid-point of the HMA. Interestingly, the small concave shape discussed previously appears at the interface of the HMA and underlying layer. As stated previously, it was hypothesized that this small concave shape could be a crack within an underlying CSM layer. For the longitudinal crack described in Figures 45 and 46, there was an underlying CSM layer. However, as shown within the lower left photograph of Figure 46, there was not a crack in the location that the core was cut.

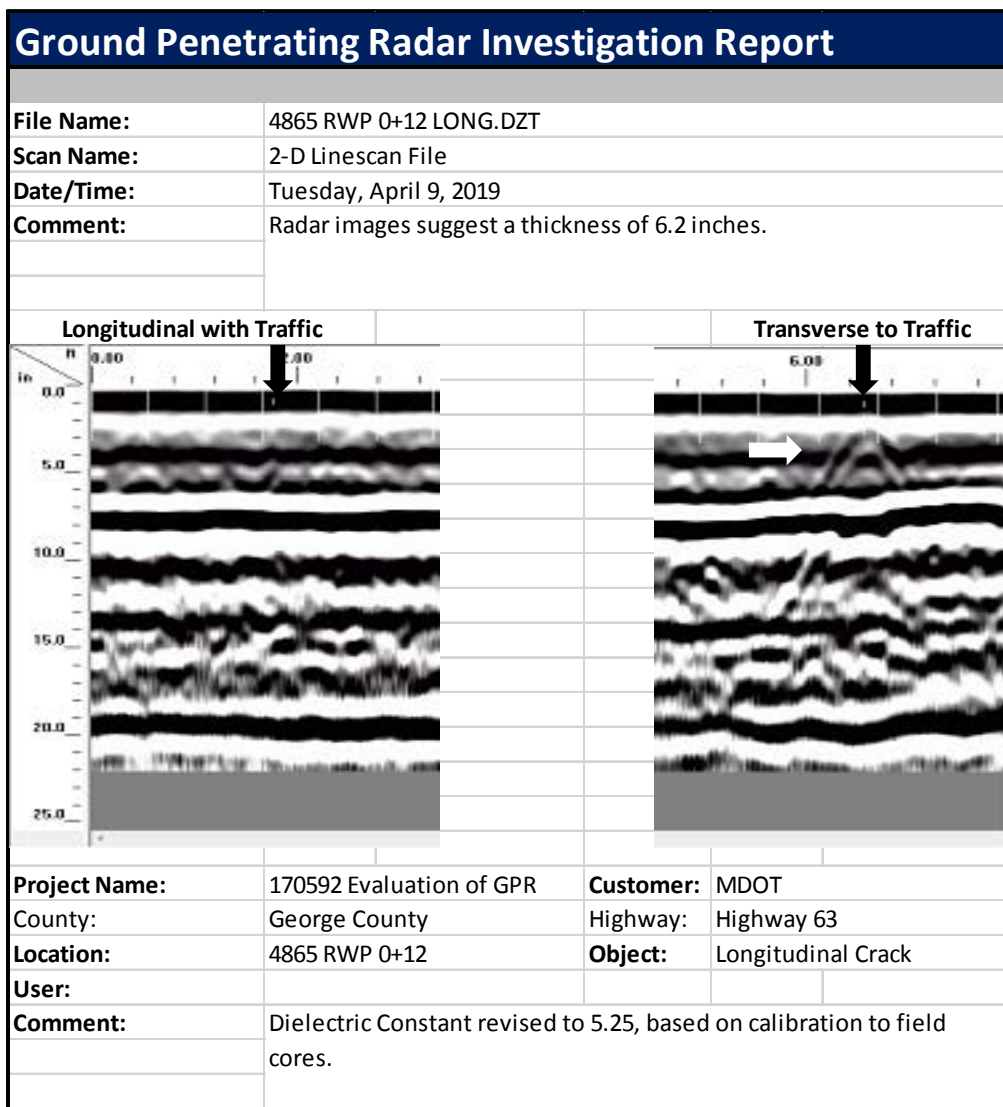


Figure 45: GPR Trace for Longitudinal Crack - Section 4865, Station 0+12



Figure 46: Pavement Surface and Core for Longitudinal Crack - Section 4865, Station 0+12

Figure 47 presents the last example of GPR traces for longitudinal cracks. These traces are from Section 5627 near station 2+16. As shown within the figure, the transverse GPR trace shows the characteristic parabola indicating the longitudinal crack. Figure 48 presents photographs of the pavement surface and core from this location. The longitudinal crack is

moderate to high severity at the pavement surface. However, the photograph of the core shows that the crack extends only about 4 in. into the pavement.

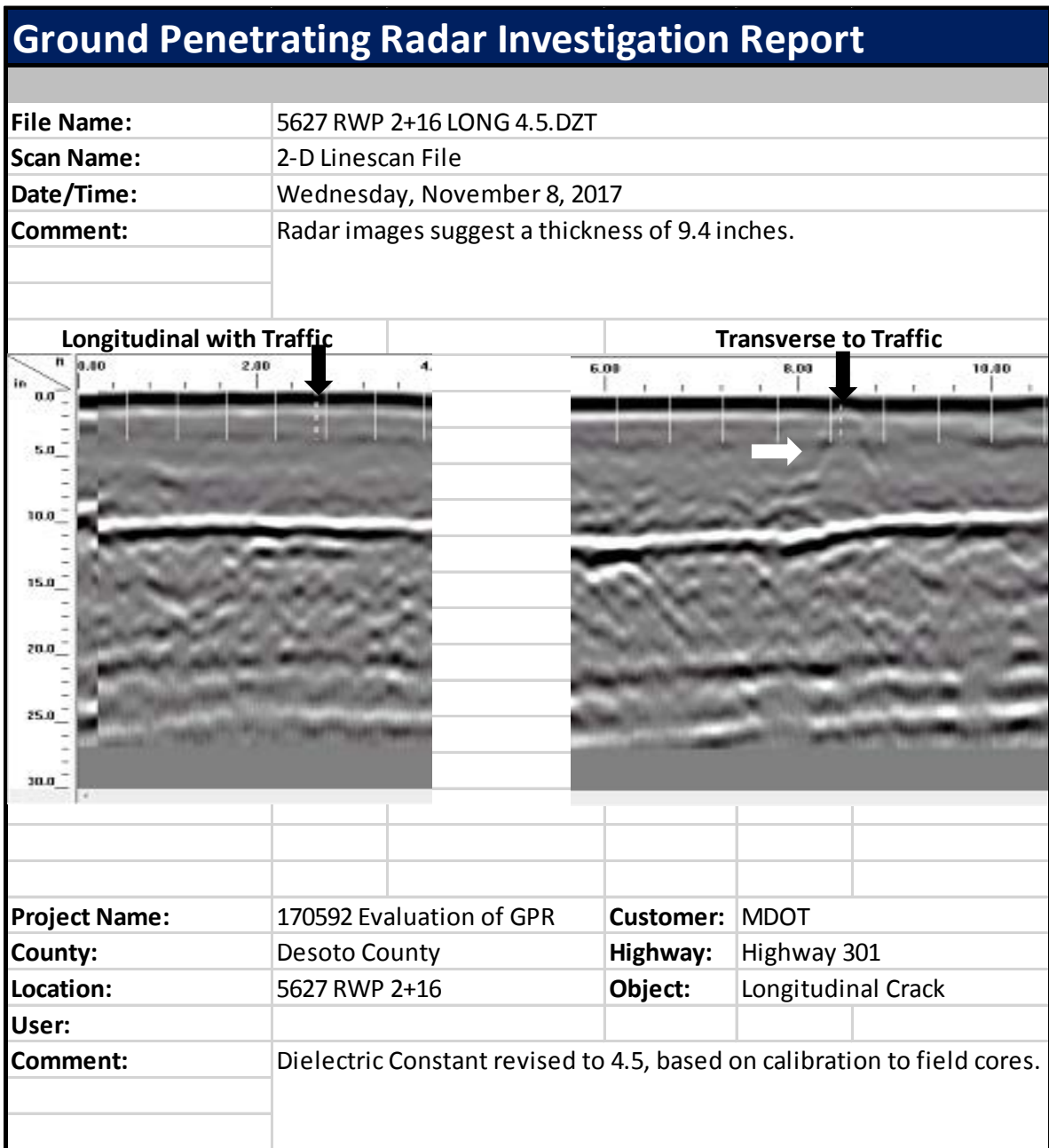


Figure 47: GPR Traces for Longitudinal Crack - Section 5627, Station 2+16



Figure 48: Pavement Surface and Core for Longitudinal Crack - Section 4865, Station 2+16

In most instances, the GPR trace was able to indicate the existence of a longitudinal crack. This indication was typically in the transverse to traffic trace. One instance where the GPR was not as successful at indicating a longitudinal crack was for low severity cracks, initiated top-down, and did not extend more than an inch or two into the pavement surface. In instances

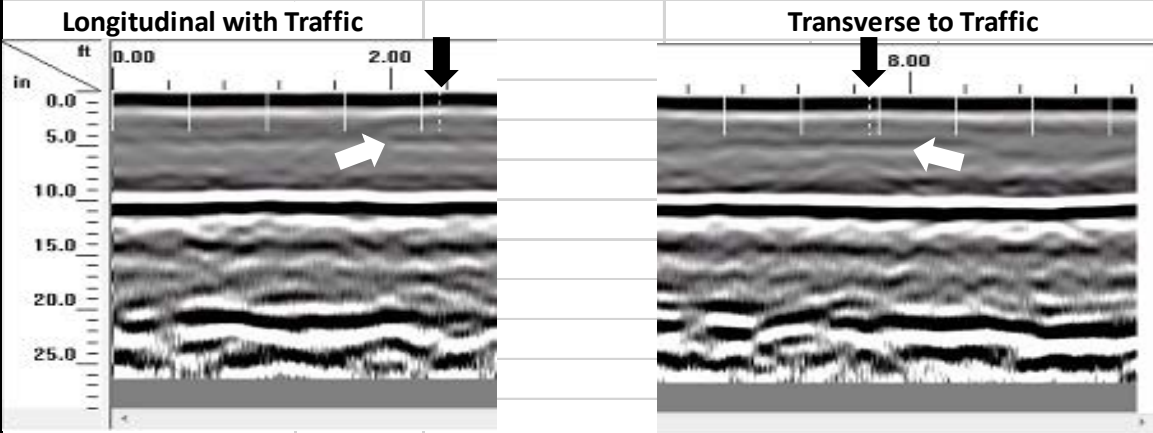
where a top-down crack extended farther into the pavement surface or had a moderate to high severity, the GPR was much more successful in identifying the existence of the crack. Though the GPR was not as successful for the relatively shallow top-down cracks, it is important to note that by not identifying the crack, the GPR trace may provide the indication that a visible low severity crack is top-down and has not propagated deep into the pavement. GPR traces were successful in identifying reflective cracks of rehabbed pavements. This is likely because the cracks are wider just below the overlay. Also, the ground-coupled GPR system tends to identify subsurface anomalies better than near-surface anomalies.

GPR Traces for Visible Transverse Cracks

Figure 49 presents the longitudinal and transverse GPR traces for a transverse crack within Section 3163 near station 3+91. Being a transverse crack, the GPR traces within the longitudinal direction would generally provide a better indication of the distress. As shown within the longitudinal trace (left trace), a faint parabola exists at the location of the crack. Another characteristic within both the longitudinal and transverse traces are shaded, gray lines (see white arrows on traces) at a depth of about 5 in. It was hypothesized earlier in this report that these shaded, gray lines could indicate stripping or delamination.

Ground Penetrating Radar Investigation Report

File Name:	3163 BWP 3+91 TRANS.DZT
Scan Name:	2-D Linescan File
Date/Time:	Tuesday, December 12, 2017
Comment:	Radar images suggest a thickness of 9.1 inches



Project Name:	170592 Evaluation of GPR	Customer:	MDOT
County:	Franklin County	Highway:	Highway 84
Location:	3163 BWP 3+91	Object:	Transverse Crack
User:			
Comment:	Dielectric Constant revised to 4.8, based on calibration to field cores.		

Figure 49: GPR Traces for Transverse Crack - Section 3163, Station 3+91

Figure 50 presents photographs of the pavement surface and the core obtained from this location. As shown in Figure 50, the transverse crack had a low severity. The core from this location shows that the crack was top-down and extended only an inch or two into the pavement. Delamination and stripping had occurred below the surface layer of HMA as well as just above the bottom layer of HMA.



Figure 50: Pavement Surface and Core for Transverse Crack - Section 3163, Station 3+91

Figure 51 illustrates the GPR traces for a transverse crack within Section 4782 at station 1+63. Within the longitudinal trace, a distinct parabola exists below the visible distress. Additional anomalies are below the top parabola including a parabola near the interface between the HMA and underlying CSM layer.

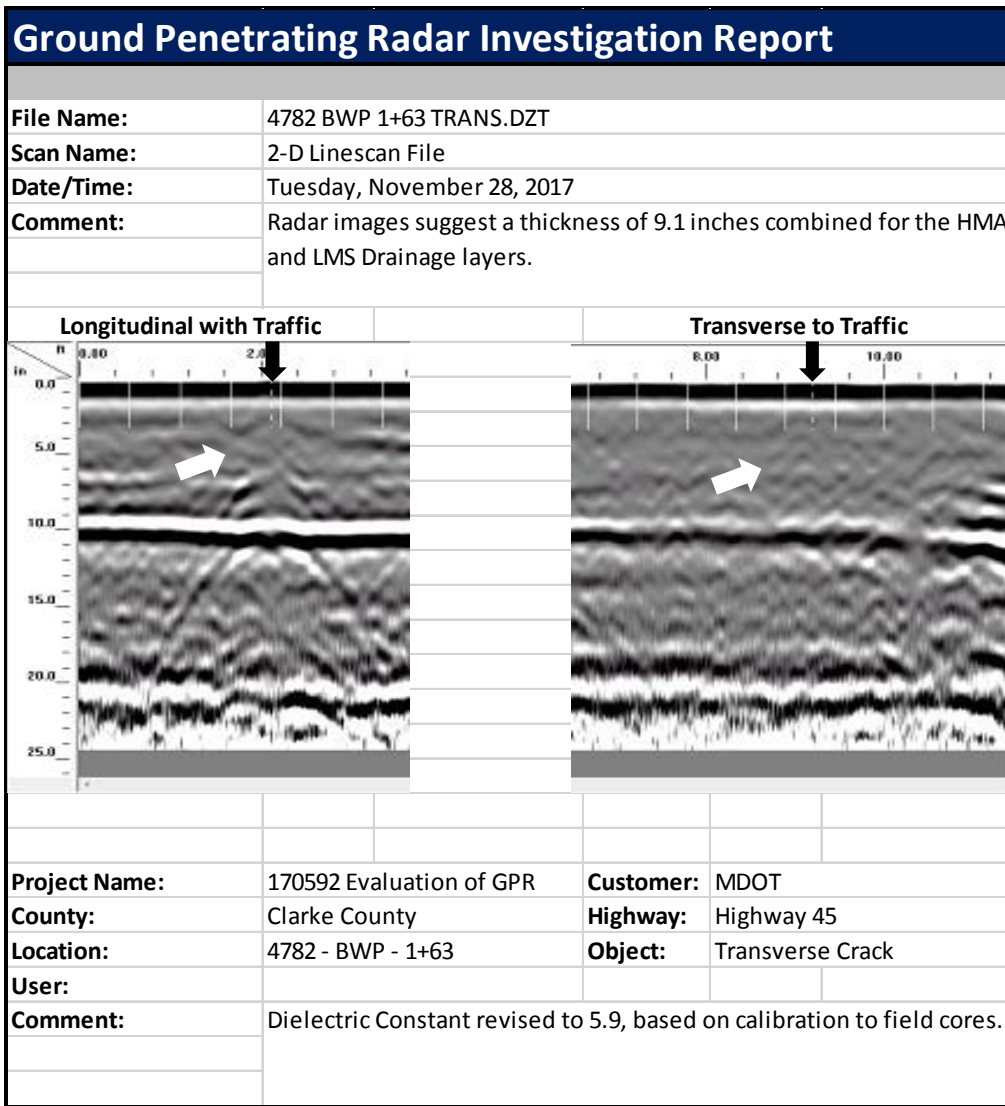


Figure 51: GPR Traces for Transverse Crack - Section 4782, Station 1+63

Figure 52 presents photographs of the pavement surface and core obtained at the location of the Figure 51 GPR traces. As shown in this figure, the transverse crack extended across the entire pavement lane. The core cut from this location (bottom right photograph of Figure 52) shows that the crack extended through the entire HMA layer. However, a crack was not found within the CSM layer at the location of the core.

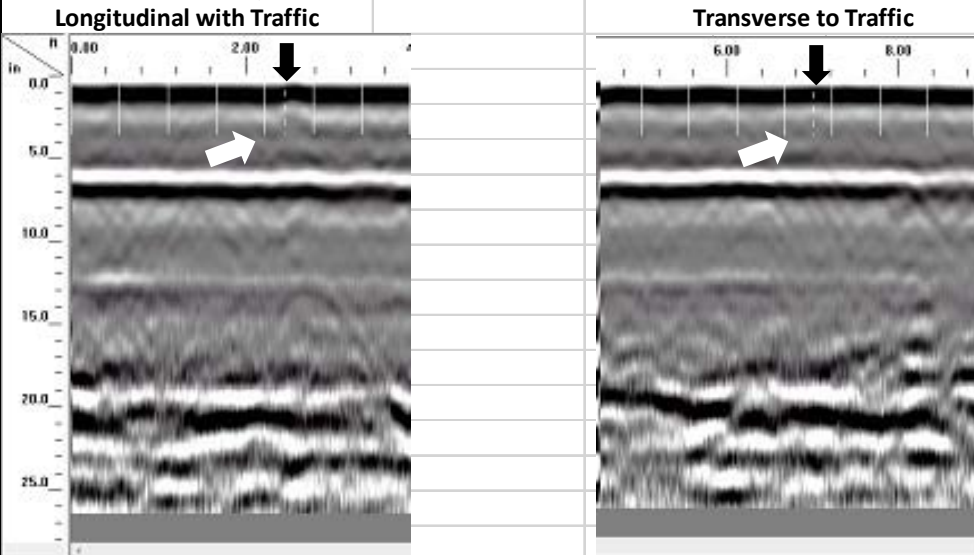


Figure 52: Pavement Surface and Core from Transverse Crack - Section 4782, Station 1+63

GPR traces of a transverse crack from Section 4784 near station 0+15 are illustrated within Figure 53. The longitudinal trace shows an anomaly directly under the location of the distress. The parabola is somewhat faint, but does exist.

Ground Penetrating Radar Investigation Report

File Name:	4784 BWP 0+15 TRANS.DZT
Scan Name:	2-D Linescan File
Date/Time:	Wednesday, November 29, 2017
Comment:	Radar images suggest a thickness of 5.7 inches



Project Name:	170592 Evaluation of GPR	Customer:	MDOT
County:	Clarke County	Highway:	Highway 45
Location:	4784 BWP 0+15	Object:	Transverse Crack
User:			
Comment:	Dielectric Constant revised to 5.1, based on calibration to field cores.		

Figure 53: GPR Traces for Transverse Crack - Section 4784, Station 0+15

Figure 54 presents photographs from station 0+15 of Section 4784. As shown within these photos, the transverse crack was low severity and was BWP. Based on the photograph of the core, the transverse crack was top-down that extended through about half of the HMA layer. The CSM layer below the HMA did not have a crack at the location the core was obtained.



Figure 54: Pavement Surface and Core from Transverse Crack - Section 4784, Station 0+15

The final example of comparing visible transverse cracks to GPR traces is from Section 5210 near station 3+75. Longitudinal and transverse GPR traces at this location are presented in Figure 55. This figure shows an anomaly under the location of the surface distress as shown by the white arrows on the longitudinal trace. Additionally, the longitudinal trace indicates some

further distresses below the surface. This observation is based upon the various dark and light shaded lines below the surface (as shown by the white arrows). The various dark and light lines also show up in the transverse trace. Also, of note, the characteristic concave shape exists at the interface between the HMA and CSM layer within the longitudinal trace.

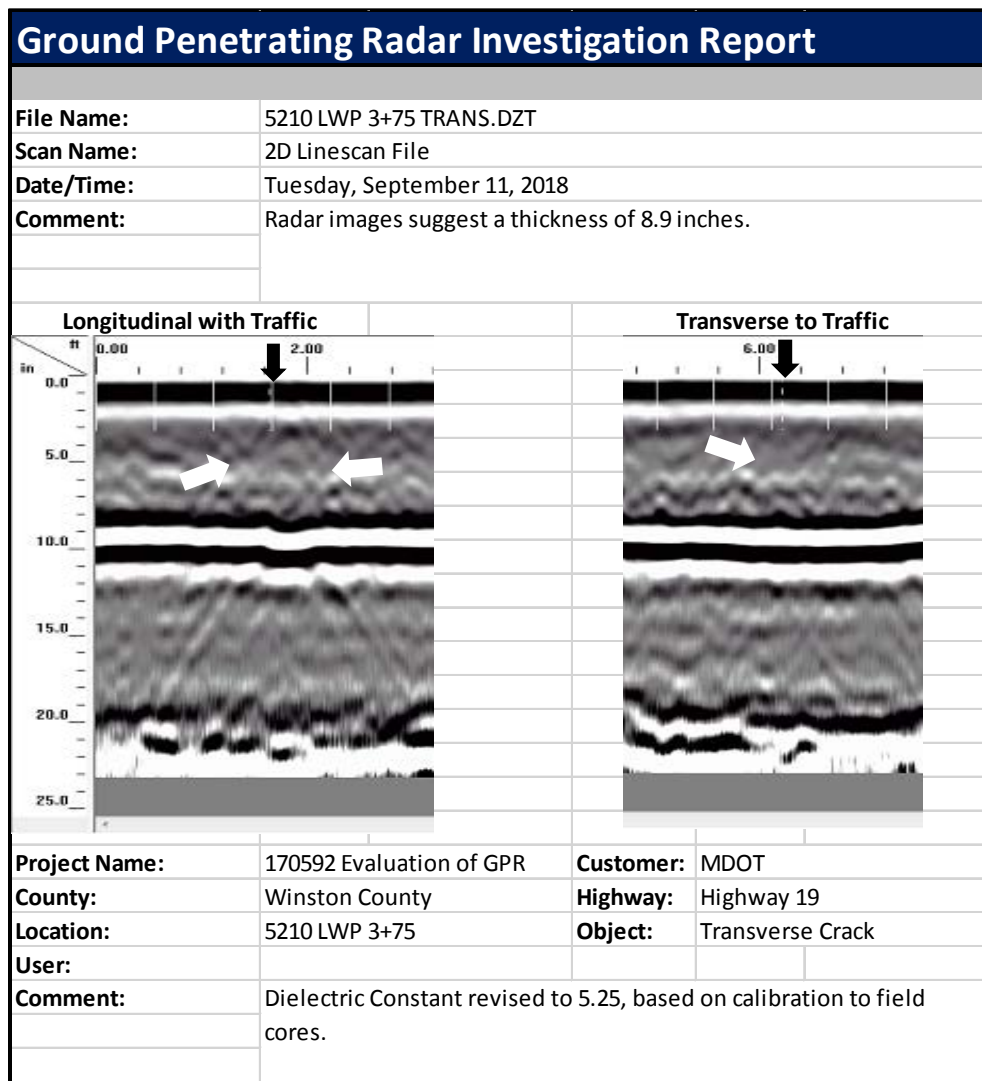


Figure 55: GPR Traces for Transverse Crack - Section 5210, Station 3+75

The pavement surface and core obtained from Section 5210 is illustrated within Figure 56. This figure shows that the crack is low to moderate severity and is BWP. Based upon the core, stripping had occurred within the middle portion of the HMA layer. The transverse crack extended from the pavement surface to the bottom of the HMA layer. Additionally, there was a crack within the CSM layer at the core location. Therefore, the various dark and light shaded lines did appear to indicate stripping (and possibly delamination) and the concave shape did appear to indicate a crack within the CSM layer.

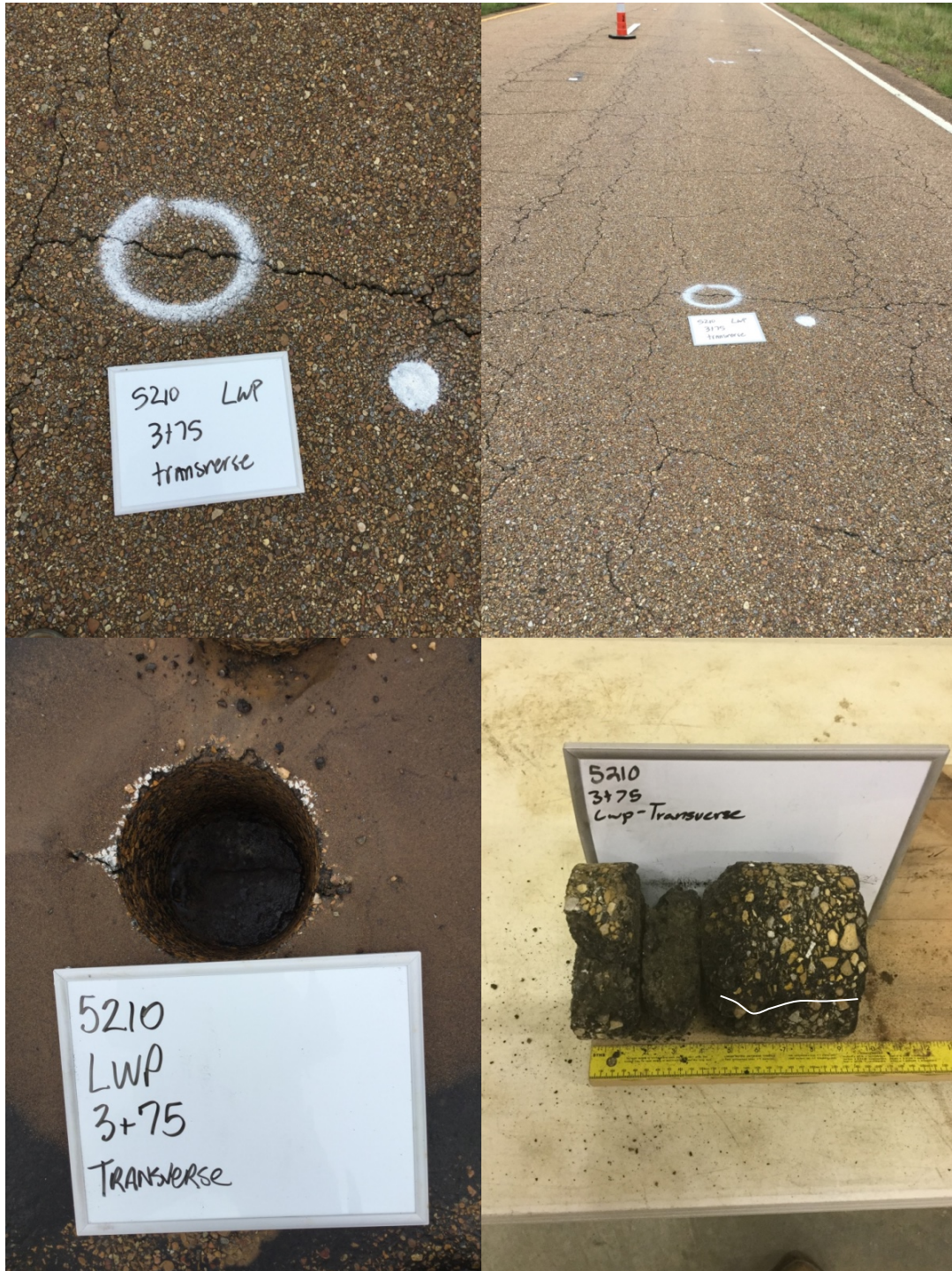


Figure 56: Pavement Surface and Core from Transverse Crack - Section 5210, Station 3+75

Similar to the longitudinal cracks, the GPR was generally successful in identifying the visible transverse cracks. In instances where the transverse crack extended to at least half the HMA layer, the GPR traces showed anomalies under the visible transverse cracks. In some

instances, the GPR traces also seemed to indicate the existence of stripping near the transverse cracks and the existence of a crack at the surface of the CSM layer.

GPR Traces of Visible Fatigue Cracking

Figure 57 shows the longitudinal and transverse GPR Traces for fatigue cracks observed within Section 4782 near station 4+65. Based upon the traces, very little can be discerned from the longitudinal trace. However, there are some anomalies below the surface within the transverse trace, though they are faint.

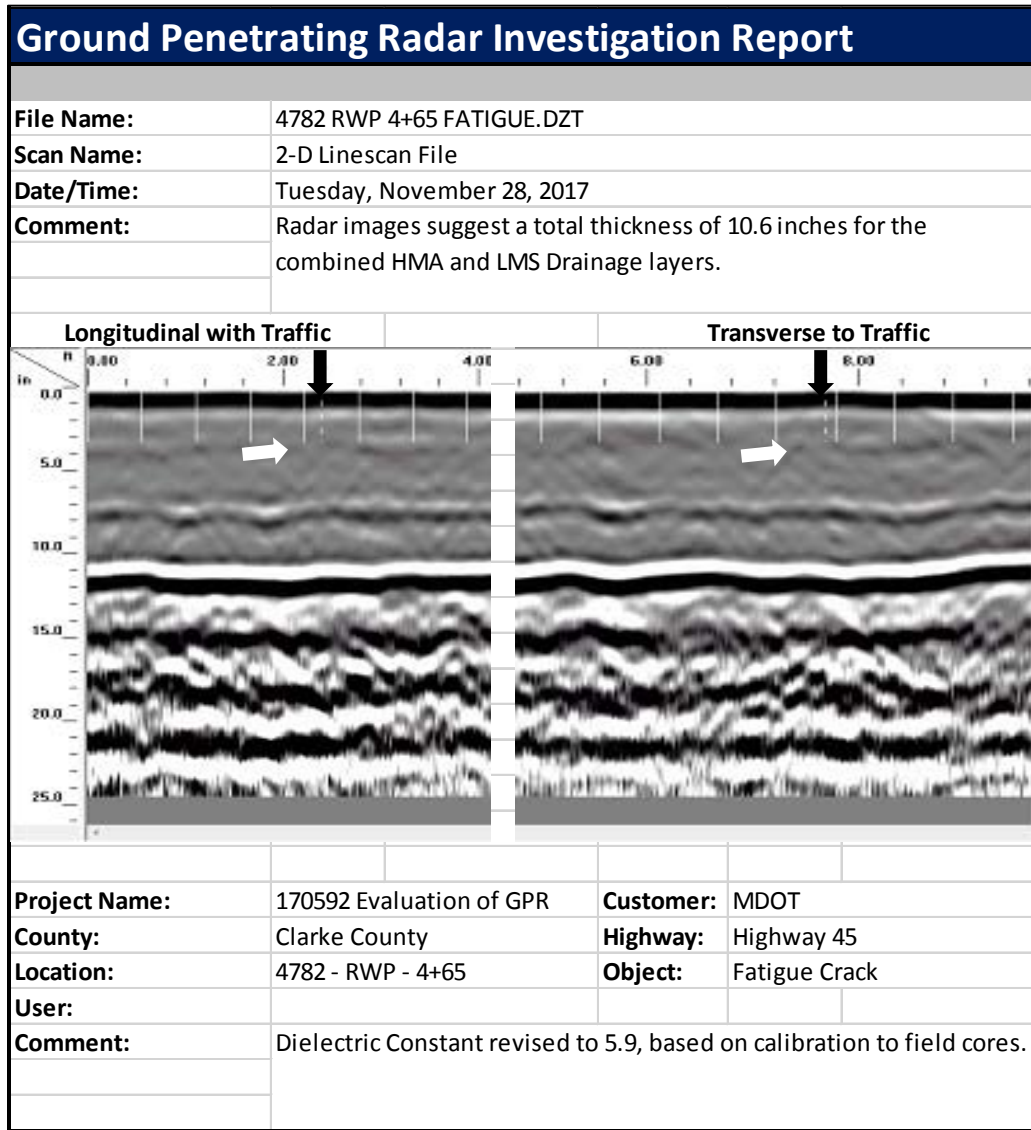


Figure 57: GPR Traces for Fatigue Cracks - Section 4782, Station 4+65

Figure 58 presents photographs of the pavement surface and a core cut from within Section 4782 at station 4+65. The fatigue cracking in this area is generally a longitudinal crack at the edge of the wheel path with secondary transverse cracks. As shown in Figure 58, the core was cut at the intersection of the longitudinal crack and one of the secondary transverse cracks. Both of these cracks would be considered low severity. The core revealed that both the longitudinal and transverse cracks extended through the entire HMA layer.



Figure 58: Pavement Surface and Core from Fatigue Cracks - Section 4782, Station 4+65

Figure 59 presents the GPR traces for fatigue cracking within Section 5230 near station 1+25. The transverse to traffic trace does appear to show an anomaly near the pavement surface (as designated by the white arrow). Interestingly, both traces show a dark shaded line at a depth of about 4 in.

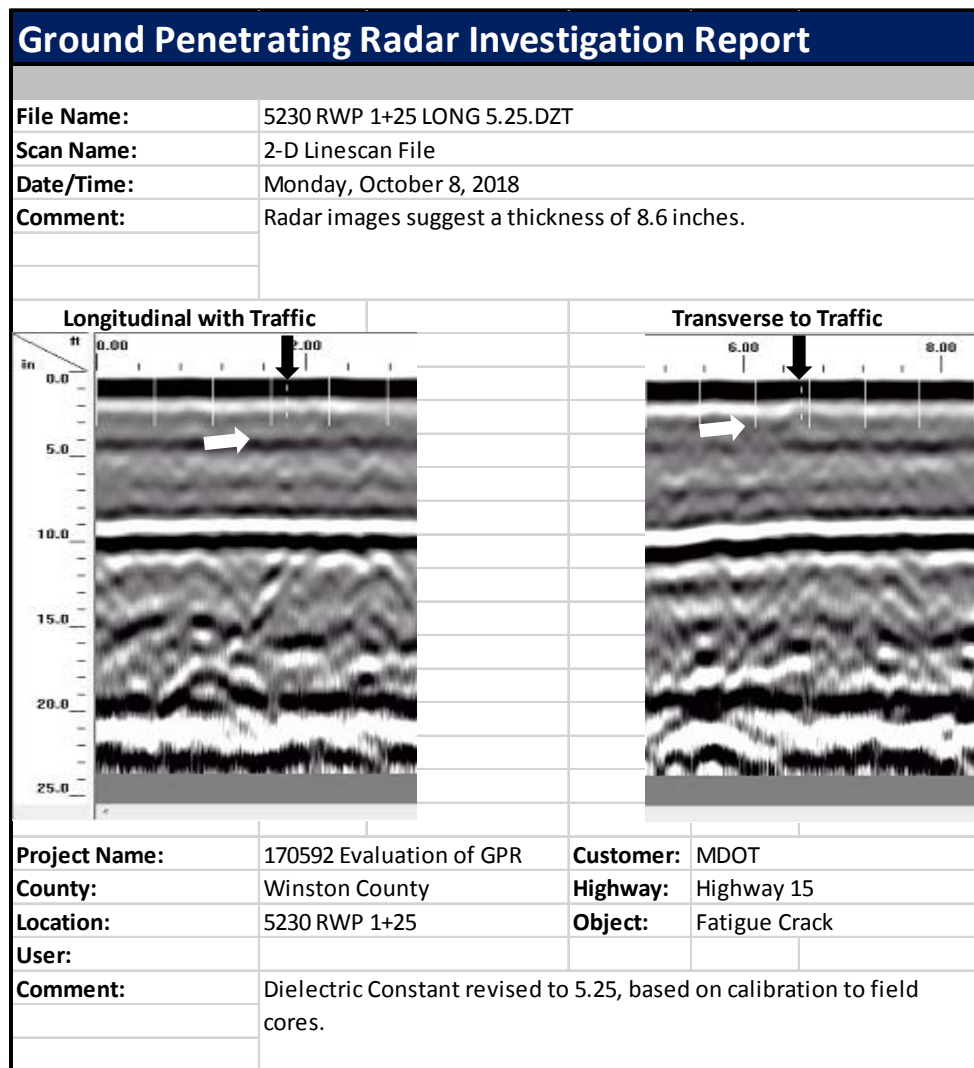


Figure 59: GPR Traces for Fatigue Cracks - Section 5230, Station 1+25

Photographs of the pavement surface and core cut from Section 5230 are presented within Figure 60. As shown within this figure, the pavement surface has the appearance of classical “alligator” cracking and are low to moderate severity. However, the core cut from the pavement indicated that the cracks only extended through the first layer of HMA. Therefore, these cracks are top-down or bottom-up from the bottom of the surface layer. The core also shows delamination and some stripping at the bottom of the HMA surface layer.



Figure 60: Pavement Surface and Core from Fatigue Crack - Section 5230, Station 1+25

Figure 61 presents the GPR traces for the final example of fatigue cracking. These traces are from Section 5249 near station 0+12. Based upon the two traces, the longitudinal trace appears to show an anomaly at the location of the surface distress (black arrow). Interestingly, another anomaly existed several feet in front of the surface distress location.



Figure 62: Pavement Surface and Core from Fatigue Crack - Section 5249, Station 0+12

The GPR traces for the visible fatigue cracking were somewhat successful. Similar to the traces for longitudinal and transverse cracks, it appears that the severity of the crack and the depth at which the crack extends into the HMA layer affect the ability of the GPR to identify visible distresses. Low severity cracks that only extend a short distance into the pavement are

not as easily identified as cracks that are more severe or extend throughout the pavement. As stated previously, this point is also important and is likely a by-product of using a ground-coupled GPR system. When the fatigue cracks extend throughout the entire of HMA, the GPR is more likely to highlight the distress.

Summary

As stated previously, the full length GPR traces were somewhat easier to evaluate than the short GPR traces conducted over the visible distresses. In most cases, the GPR traces did indicate an anomaly under the specific surface distress being evaluated. In those instances, in which the GPR did not indicate an anomaly at the surface distress, it was generally for low severity cracks that did not extend very deep into the pavement. Though the GPR was not successful in identifying these shallow top-down cracks, it is still important to note that by not identifying the distress, the GPR may be providing an indication that a visible low severity crack is top-down and has not propagated deep into the pavement. Where a top-down crack extended deeper into the pavement or the crack had propagated through the entire layer, the GPR was much more successful in indicating the distress.

Conclusions and Recommendations

The objective of this study was to evaluate whether the GPR could be used as a tool to assist an Engineer design an M&R treatment. In order to accomplish the objectives of this study, GPR testing was conducted on 64 pavement sections located throughout Mississippi. These pavement sections provided a range of pavement ages, structures, materials, and performances.

GPR testing was conducted in two different manners at each of the 64 sections. First, five GPR traces were conducted along the full 500 ft length of the pavement section. These five traces were along the right pavement edge, within the right wheel path, between the wheel paths, within the left wheel path, and along the left pavement edge (next to longitudinal joint). Secondly, GPR traces were obtained over visible distresses. Generally, four to ten visible distresses were selected for GPR evaluations. Evaluation of the visible distresses involved obtaining 2- to 3-ft traces in both the longitudinal and transverse directions. After conducting these two GPR traces, the visible distress was cored.

Using the collected data, three different analyses were conducted for 16 of the 64 sections. First, a case study was conducted for Site 4669 near Woodville, MS. The term case study is used because this section afforded the only opportunity for the evaluation of the five full length traces prior to sampling the section. This opportunity arose because of equipment issues. The second analysis technique involved evaluating the five full length traces from each

of the 16 sections to identify trace characteristics that may be subsurface distresses or other issues. The final analysis technique was to evaluate the GPR traces of selected visible distresses. Based upon the data collected and analyses conducted, the following conclusions are provided:

- In the one instance in which the traces were evaluated prior to the sampling of the pavement, the GPR successfully identified subsurface distresses. Subsurface distresses successfully identified included both cracking within the HMA and cracking within the CSM layer.
- Subsurface anomalies identified by the GPR were generally parabolas, areas of altering shades of gray, distinct lines of darker gray colors, and distortions within the interfaces between layers.
- The GPR identified subsurface anomalies that included both stripping and delamination.
- The GPR identified subsurface anomalies that could be stripping.
- Subsurface anomalies were identified based on GPR traces that indicated cracks that were near the bottom of the HMA layer.
- Subsurface anomalies were identified based on GPR traces that indicated cracks that had either: 1) initiated mid-depth within the HMA or 2) had propagated from the bottom of the HMA layer to mid-depth.
- Subsurface anomalies found within the CSM layers suggested cracks within the CSM layers.
- Distortions within interfaces between layers suggested the potential for fatigue and/or shrinkage cracks within CSM layers.
- The GPR was successful at identifying cracks visible at the pavement surface.
- One instance that the GPR did not always identify cracks visible at the pavement surface was when the cracks were low severity, top-down, and did not extend very far into the pavement. This observation is important, however, because it provides an indication that a visible surface crack is top down and shallow if the GPR does not identify the crack.
- The five full length traces proved easier to evaluate than the short traces obtained over the visible distresses. Full length traces allowed for the observation of boundaries of distinguishing anomalies within these long traces as opposed to the shorter traces where distinguishing anomalies often fully encompassed the full length of the shorter traces; i.e., no features within the shorter trace could be interpreted as a boundary between a distressed and non-distressed area of the pavement layer.
- Based upon the previous conclusions, it is concluded that the GPR does have the potential to assist an Engineer design an M&R treatment.

Based upon the conclusions of this study, the following recommendations are provided:

- Within the current study, GPR traces from 16 of the available 64 pavement sections were evaluated. Because of the success of identifying anomalies within the traces,

and the success, where available, of correlating GPR traces to actual subsurface distresses, it is recommended to evaluate the GPR traces from the remaining 48 sections. Both full length and individual surface distress traces should be evaluated. Evaluation of the remaining GPR traces from the remaining 48 sections may provide further evidence of the ability of the GPR to assist an Engineer design an M&R treatment.

- After evaluating the remaining 48 sections, a subset of the 64 sections should be selected for further investigation. To date, only a single section afforded the opportunity to evaluate the traces and then sample the pavements to verify that the subsurface anomalies were in fact distresses. A minimum of five additional sections should be sampled for verification purposes.

Implementation Plan/Recommendations

The findings of this study, though successful, are not implementable at this point. The research did show the potential for use of the GPR during the design of an M&R treatment; however, additional research is needed to verify that the anomalies found are in fact subsurface distresses or issues.

References

1. Uddin, W. "Ground Penetrating Radar Study – Phase I: Technology Review and Evaluation." Report No. FHWA/MS-DOT-RD-06-182. Mississippi Department of Transportation. Jackson, MS. August 2006.
2. Miller, J.S. and W.Y. Bellinger. "Distress Identification Manual for the Long-Term Pavement Performance Program." Report No. FHWA-ED-03-031. Fourth Revised Edition. Federal Highway Administration. Washington, D.C. June 2003.
3. Scullion, T. and T. Saarenketo. "Applications of Ground Penetrating Radar Technology for Network and Project Level Pavement Management Systems." 4th International Conference on Managing Pavements. Pretoria, South Africa. 1998.